New insights into widely linear MMSE receivers for communication networks using data-like rectilinear or quasi-rectilinear signals -Part II: three-inputs receivers

Pascal Chevalier, Jean-Pierre Delmas, Roger Lamberti

New insights into widely linear MMSE receivers for communication networks using data-like rectilinear or quasi-rectilinear signals - Part II: three-inputs receivers

Pascal Chevalier, Jean-Pierre Delmas, and Roger Lamberti

***Abstract*—Widely linear (WL) processing has raised up a great interest since nearly three decades for multi-user (MUI) interference mitigation in radiocommunications networks using rectilinear (R) or quasi-rectilinear (QR) signals in particular. This topic remains of interest for many current applications using R or QR signals such as anti-collisions in Radio Frequency Identification (RFID) or satellite-AIS systems, grant free massive access in NB-IOT networks, multipaths mitigation in the Control and Non Payload Communications (CNPC) link of Unmanned Aerial Vehicle (UAV) or FBMC-OQAM networks. Most of WL receivers currently available for MUI mitigation are WL MMSE receivers implemented at the symbol rate after a matched filtering operation to the pulse shaping filter. These WL receivers have thus a particular structure constraint which prevents them from exploiting the cyclostationarity of the data-like MUI and which makes them suboptimal within the WL MMSE receivers. For this reason, two alternative WL MMSE receivers, without any structure constraint and exploiting or not the cyclostationarity of the MUI have been computed and analyzed in the companion paper [2]. The first one is the optimal one, which requires the a priori knowledge or estimation of the MUI channels, which may be cumbersome in practice. The second one does not require the a priori knowledge of the MUI channels, is quasi-optimal for R signals and small bandwidth but remains suboptimal otherwise. In this context, to improve the performance of the latter receiver while keeping its advantages, the purpose of this paper is to propose, for both R and QR signals, a new WL MMSE receiver, called three-input WL FRESH MMSE receiver, and to analyze, both analytically and by computer simulations, its performance. This new receiver is shown to be quasi-optimal in most situations and open new perspective for implementation optimization of WL MMSE receivers and for the implementation of the optimal receiver from the only knowledge of the SOI channel.**

***Index Terms*—Non circular, widely linear, MMSE, rectilinear, quasi-rectilinear, SAIC/MAIC, MUI, MAI, ISI, ICI, continous-time, FRESH, GMSK, OQAM, ASK, PSK, QAM, Beyond5G, AIS, FBMC, UAV, CNPC.**

P. Chevalier is with CNAM, laboratoire CEDRIC, HESAM University, 292 rue Saint Martin, 75141 Paris Cedex 3, France and also with Thales France, HTE/AMS/TCP, 4 Av. Louvresses, 92622 Gennevilliers, Cedex, France e-mail: pascal.chevalier@cnam.fr, pascal.chevalier@thalesgroup.com.

J.-P. Delmas is with Samovar laboratory, Telecom SudParis, Institut Polytechnique de Paris, 91120 Palaiseau, France, e-mail: jean-pierre.delmas@it-sudparis.eu.

R. Lamberti is with CITI department, Telecom SudParis, Institut Polytechnique de Paris, 91120 Palaiseau, France, e-mail: roger.lamberti@mines-telecom.fr.

Paper submitted to IEEE Trans. Vehicular Technology

I. Introduction

WIDELY linear (WL) processing [1] has raised up a great interest since nearly three decades for multi-user interference (MUI) and multi-antenna interference (MAI) mitigation in radio-communication networks using rectilinear (R) or quasi-rectilinear (QR) modulations in particular. Definition of R and QR signals, jointly with numerous papers about MUI mitigation by WL processing in radiocommunications networks may be found in the companion paper [2]. However, despite these numerous papers, this topic remains of great interest for several current and future applications. Among the latter we may cite anti-collisions processing in Radio Frequency Identification systems [3] or in dense machine-type networks such as grant-free narrow-band Internet of Things (IoT) networks for uplink transmissions [4], which use R and QR signals respectively, and in satellite-AIS systems for maritime surveillance which use GMSK signals [5]–[7]. Another application corresponds to 5G and Beyond 5G (B5G) networks, where WL processing may allow to support a massive number of low data rate devices through one-dimensional signaling [8], [9], potentially jointly with MIMO non-orthogonal multiple access (MIMO-NOMA) systems [10], or fully or overloaded large MU-MIMO systems using R signals [11]. Moreover, as explained in [2], QR interference mitigation by WL processing remains also of great interest for the bidirectional Control and Non Payload Communications (CNPC) link of Unmanned Aerial Vehicles (UAVs or drones), which uses the GMSK modulation [12], and for networks which use FBMC-OQAM waveforms [13], which are candidate for B5G and future Internet of Things networks [14].

In this stimulating context, we must note that most of the WL receivers, which have been developed in the literature for R or QR MUI mitigation, correspond to a WL MMSE

receiver which is implemented at the symbol rate, after a matched filtering operation to the pulse shaping filter. This WL MMSE receiver has thus a particular structure constraint (see [2] and reference herein) and is denoted by (sc) WL MMSE receiver in [2] and this paper. It has been shown in [2] that this (sc) WL MMSE receiver is generally suboptimal within the WL MMSE receivers, for frequency selective channels in particular but also for channels without any delay spread, since the structure constraint prevents them to exploit the cyclostationarity of the data-like MUI in particular. For this reason, using a continuous-time (CT) approach, whose advantages have been presented in [2], two alternative WL MMSE receivers, without any structure constraint, have been computed and analyzed in [2], in presence or absence of data-like MUI, for both R and QR signals. The first one, denoted by (o) WL MMSE receiver, corresponds to the optimal WL MMSE receiver. It fully exploits the cyclostationarity properties of the MUI but its implementation requires the a priori knowledge or estimation of the MUI channels, which may be cumbersome in practice. The second one, denoted by (s) WL MMSE receiver, does not exploit the cyclostationarity of the MUI by falsely assuming them as stationary. This receiver is very interesting in practice since it does not require the a priori knowledge or estimation of the MUI channels. In the absence of interference, it has been shown in [2] that the (o) and (s) WL MMSE receivers coincide and outperform the (sc) WL MMSE receiver for frequency selective channels, hence their great interest. In the presence of interference and for R signal of interest (SOI) and data-like MUI, the (s) WL MMSE receiver has been shown in [2] to be quasi-equivalent to the (sc) WL MMSE receiver for channels with no delay spread and quasi-optimal (and thus quasi-equivalent to the (o) WL MMSE receiver) for reduced bandwidth, but with an increasing sub-optimality as the bandwidth increases. However, for QR SOI and data-like MUI, the (s) WL MMSE receiver has been shown in [2] to be less powerful than the (sc) WL MMSE receiver for channels with no delay spread and always sub-optimal whatever the bandwidth. This different results obtained for R and QR signals show in particular the non-equivalence of R and QR signals for WL MMSE receivers, results which has already been obtained in [15], [16] for WL pseudo-MLSE receivers without and with frequency offsets.

To improve, for both R and QR signals, the performance of the (s) WL MMSE receiver in the presence of data-like MUI, while keeping its advantages, we propose in this paper, through the CT approach presented in [2], an extended (s) WL MMSE receiver corresponding to a (s) three-input WL frequency shifted (FRESH) MMSE receiver, denoted by (s) three-input WL MMSE receiver in this paper. This receiver, which exploits the SO cyclostationarity of the MUI, has no structure or architecture constraint, excepted its three-input structure, and does not require the a priori knowledge or estimation of the MUI channels, hence its great interest for practical implementations. Note that a three-input WL receiver has already been proposed in [15], [16] for QR signals but using a pseudo-MLSE approach instead of a MMSE one. It is shown in this paper, both analytically and by computer simulations, that for both R and QR signals, the (s) three-input WL MMSE receiver is quasi-optimal in the absence and presence of data-like MUI for most of pulse shaping filters, constellations and propagation channels. This interesting result open new perspectives for the implementation optimization of WL MMSE receivers in the presence of data-like MUI and, in particular, for the implementation of (o) WL MMSE receivers from the only knowledge of the SOI channel.

The paper is organized as follows. Section II recalls the observation model and the extended one, introduced in [2], for standard two-input WL processing of both R and QR signals. Section III recalls, for R and QR signals, the expressions of (o), (s) and (sc) L and standard two-input WL MMSE receivers computed in [2]. Section IV introduces, for both R and QR signals, the (s) three-input WL MMSE receiver and gives a general closed-form expression of the SINR on the current symbol at the real-part output of this receiver. Section V analyses, both analytically and by computer simulations, the performance of the (s) three-input WL MMSE receiver, in terms of output SINR, in the presence of one data-like MUI and compares this performance to that of the (o), (s) and (sc) two-input WL MMSE receivers. Section VI shows that the results obtained through the output SINR criterion are still valid for the output symbol error rate (SER). Finally section VII concludes this paper.

Notations: Before proceeding, we fix the notations used throughout the paper. Non boldface symbols are scalar whereas lower (upper) case boldface symbols denote column vectors (matrices). T, H and $*$ means the transpose, conjugate transpose and conjugate, respectively. $\otimes$ is the convolution operation. $\mathbf{0}_{K,L}$ and $\mathbf{I}_K$ are the zero and the identity matrices of dimension $K \times L$ and K, respectively and $\mathbf{J}_{2K}$ is the $2K \times 2K$ exchange matrix. $\delta(x)$ is the Kronecker symbol such that $\delta(x) = 1$ for $x = 0$ and $\delta(x) = 0$ for $x \neq 0$. Moreover, all Fourier transforms of vectors $\mathbf{x}$ and matrices $\mathbf{X}$ use the same notation where time parameters t or τ is simply replaced by frequency f.

II. Models and extended ones for two-input WL processing

A. Observation model

We recall in this section the observation model introduced in [2]. More precisely, we consider an array of N narrowband antennas receiving the contribution of a R or QR SOI, P data-like MUI and a background noise. The $N \times 1$ vector of complex amplitudes of the data at the output of these antennas after frequency synchronization can then be written

as

$$\mathbf{x}(t) = \sum_{\ell} a_\ell \mathbf{g}(t-\ell T) + \sum_{1\le p\le P}\sum_{\ell} a_{p,\ell}\mathbf{g}_p(t-\ell T)+\boldsymbol{\epsilon}(t) = \sum_{\ell}\mathbf{G}(t-\ell T)\mathbf{a}_\ell+\boldsymbol{\epsilon}(t) \stackrel{\text{def}}{=} \sum_{\ell} a_\ell \mathbf{g}(t-\ell T)+\mathbf{n}(t) \quad (1)$$

Here, $(a_\ell, a_{p,\ell}) = (b_\ell, b_{p,\ell})$ for R signals, whereas $(a_\ell, a_{p,\ell}) = (j^\ell b_\ell, j^\ell b_{p,\ell})$ for QR signals, where b_ℓ and $b_{p,\ell}$, $1 \le p \le P$ are real-valued zero-mean independent identically distributed (i.i.d.) random variables, corresponding to the SOI and MUI p symbols respectively for R signals and directly related to the SOI and MUI p symbols, respectively for QR signals, T is the symbol period for R, $\pi/2$-BPSK, $\pi/2$-ASK, MSK and GMSK signals and half the symbol period for OQAM signals, $\mathbf{g}(t) = v(t) \otimes \mathbf{h}(t)$ is the $N \times 1$ impulse response vector of the SOI global channel, $v(t)$ and $\mathbf{h}(t)$ are respectively the scalar and $N \times 1$ impulse responses of the SOI pulse shaping filter and propagation channel, respectively, $\mathbf{g}_p(t) \stackrel{\text{def}}{=} v(t) \otimes \mathbf{h}_p(t)$ where $\mathbf{h}_p(t)$ is the impulse response vector of the propagation channel of the MUI p, $\mathbf{G}(t)$ is the $N \times (P+1)$ matrix defined by $\mathbf{G}(t) \stackrel{\text{def}}{=} [\mathbf{g}(t), \mathbf{g}_1(t), ..., \mathbf{g}_p(t)] = v(t) \otimes \mathbf{H}(t)$ where $\mathbf{H}(t) \stackrel{\text{def}}{=} [\mathbf{h}(t), \mathbf{h}_1(t), ..., \mathbf{h}_p(t)]$, $\mathbf{a}_\ell$ is the $(P+1)\times 1$ vector defined by $\mathbf{a}_\ell \stackrel{\text{def}}{=} [a_\ell, a_{1,\ell}, ..., a_{p,\ell}]^T$, $\boldsymbol{\epsilon}(t)$ is the $N \times 1$ background noise vector assumed to be zero-mean, circular, stationary, temporally and spatially white and $\mathbf{n}(t)$ is the total noise vector composed of the P MUI and background noise. Note that model (1) with $(a_\ell, a_{p,\ell}) = (j^\ell b_\ell, j^\ell b_{p,\ell})$ is exact for $\pi/2$-BPSK, $\pi/2$-ASK, MSK and OQAM signals whereas it is only an approximated model for GMSK signals.

For R signals, the filter $v(t)$ is assumed to correspond to a normalized (with unit-energy) square root raised cosine (SRRC) filter with a roll-off ω and a bandwidth $B = (1+\omega)/T$. For QR signals, four normalized filters $v(t)$ are considered, depending on the QR constellation. For $\pi/2$-BPSK or $\pi/2$-ASK constellations, $v(t)$ is the same as for R signals. For OQAM signals, $v(t)$ is also a normalized SRRC filter but for the symbol duration $2T$ instead of T. For a MSK signal, $v(t)$ is defined by

$$v(t) = \begin{cases} \frac{1}{\sqrt{T}}\sin(\frac{\pi t}{2T}), & t \in [0, 2T] \\ 0, & \text{elsewhere,} \end{cases} \quad (2)$$

whereas for a GMSK signal, $v(t)$ is, ideally, approximately defined by the $c_0(t)$ pulse of the Laurent decomposition [17]. However, as $c_0(t)$ is a complicate function of t, in this paper we approximate this pulse by the following Gaussian filter

$$v(t) \approx \frac{1}{(\sigma T\sqrt{2\pi})^{1/2}}\, e^{-\frac{(t-2T)^2}{4(\sigma T)^2}}, \quad (3)$$

where σ has to be chosen to approximate $c_0(t)$. The value $\sigma = 1$ seems to be a good choice [18].

B. Extended models for standard or two-input WL processing

For R signals, a standard or two-input WL processing of $\mathbf{x}(t)$ linearly processes the extended two-input model $\widetilde{\mathbf{x}}(t) \stackrel{\text{def}}{=} [\mathbf{x}^T(t), \mathbf{x}^H(t)]^T$, defined by

$$\widetilde{\mathbf{x}}(t) = \sum_{\ell}\widetilde{\mathbf{G}}(t-\ell T)\mathbf{b}_\ell + \widetilde{\boldsymbol{\epsilon}}(t) = \sum_{\ell} b_\ell \widetilde{\mathbf{g}}(t-\ell T) + \widetilde{\mathbf{n}}(t), \quad (4)$$

where $\widetilde{\boldsymbol{\epsilon}}(t) \stackrel{\text{def}}{=} [\boldsymbol{\epsilon}^T(t), \boldsymbol{\epsilon}^H(t)]^T$, $\widetilde{\mathbf{n}}(t) \stackrel{\text{def}}{=} [\mathbf{n}^T(t), \mathbf{n}^H(t)]^T$, $\widetilde{\mathbf{G}}(t) \stackrel{\text{def}}{=} [\widetilde{\mathbf{g}}(t), \widetilde{\mathbf{g}}_1(t), .., \widetilde{\mathbf{g}}_P(t)]$, $\widetilde{\mathbf{g}}(t) \stackrel{\text{def}}{=} [\mathbf{g}^T(t), \mathbf{g}^H(t)]^T$, $\widetilde{\mathbf{g}}_p(t) \stackrel{\text{def}}{=} [\mathbf{g}_p^T(t), \mathbf{g}_p^H(t)]^T$, $1 \le p \le P$, and $\mathbf{b}_\ell \stackrel{\text{def}}{=} [b_\ell, b_{1,\ell}, ...b_{P,\ell}]^T$.

For QR signals, a derotation preprocessing of the data is required before standard WL filtering. Using (1) for QR signals, the derotated observation vector can be written as

$$\mathbf{x}_d(t) \stackrel{\text{def}}{=} j^{-t/T}\mathbf{x}(t) = \sum_{\ell}\mathbf{G}_d(t-\ell T)\mathbf{b}_\ell + \boldsymbol{\epsilon}_d(t) = \sum_{\ell} b_\ell \mathbf{g}_d(t-\ell T) + \mathbf{n}_d(t), \quad (5)$$

where $\boldsymbol{\epsilon}_d(t) \stackrel{\text{def}}{=} j^{-t/T}\boldsymbol{\epsilon}(t)$, $\mathbf{n}_d(t) \stackrel{\text{def}}{=} j^{-t/T}\mathbf{n}(t)$, $\mathbf{G}_d(t) \stackrel{\text{def}}{=} [\mathbf{g}_d(t), \mathbf{g}_{1,d}(t), .., \mathbf{g}_{P,d}(t)] = v_d(t) \otimes \mathbf{H}_d(t)$, $\mathbf{g}_d(t) \stackrel{\text{def}}{=} j^{-t/T}\mathbf{g}(t)$, $\mathbf{g}_{p,d}(t) \stackrel{\text{def}}{=} j^{-t/T}\mathbf{g}_p(t)$, $v_d(t) \stackrel{\text{def}}{=} j^{-t/T}v(t)$, $\mathbf{H}_d(t) \stackrel{\text{def}}{=} [\mathbf{h}_d(t), \mathbf{h}_{1,d}(t), .., \mathbf{h}_{P,d}(t)]$, $\mathbf{h}_d(t) \stackrel{\text{def}}{=} j^{-t/T}\mathbf{h}(t)$ and $\mathbf{h}_{p,d}(t) \stackrel{\text{def}}{=} j^{-t/T}\mathbf{h}_p(t)$. Note that the derotation operation might also be defined by $\mathbf{x}_d(t) \stackrel{\text{def}}{=} j^{t/T}\mathbf{x}(t)$. A standard or two-input WL processing of QR signals, linearly processes the extended two-input derotated model $\widetilde{\mathbf{x}}_d(t) \stackrel{\text{def}}{=} [\mathbf{x}_d^T(t), \mathbf{x}_d^H(t)]^T$, defined by

$$\widetilde{\mathbf{x}}_d(t) = \sum_{\ell}\widetilde{\mathbf{G}}_d(t-\ell T)\mathbf{b}_\ell + \widetilde{\boldsymbol{\epsilon}}_d(t) = \sum_{\ell} b_\ell \widetilde{\mathbf{g}}_d(\ell T) + \widetilde{\mathbf{n}}_d(t), \quad (6)$$

where $\widetilde{\boldsymbol{\epsilon}}_d(t) \stackrel{\text{def}}{=} [\boldsymbol{\epsilon}_d^T(t), \boldsymbol{\epsilon}_d^H(t)]^T$, $\widetilde{\mathbf{n}}_d(t) \stackrel{\text{def}}{=} [\mathbf{n}_d^T(t), \mathbf{n}_d^H(t)]^T$, $\widetilde{\mathbf{G}}_d(t) \stackrel{\text{def}}{=} [\widetilde{\mathbf{g}}_d(t), \widetilde{\mathbf{g}}_{1,d}(t), .., \widetilde{\mathbf{g}}_{P,d}(t)]$, $\widetilde{\mathbf{g}}_d(t) \stackrel{\text{def}}{=} [\mathbf{g}_d^T(t), \mathbf{g}_d^H(t)]^T$ and $\widetilde{\mathbf{g}}_{p,d}(t) \stackrel{\text{def}}{=} [\mathbf{g}_{p,d}^T(t), \mathbf{g}_{p,d}^H(t)]^T$, $1 \le p \le P$.

C. M-input generic model for L and standard WL processing

In the following, we consider L and WL receivers as one and two-input receivers, respectively. Then, for the M-input MMSE receivers ($M = 1, 2$), we denote by $\mathbf{x}_M(t)$ the generic observation vector. For linear receivers ($M = 1$), $\mathbf{x}_M(t)$ reduces to $\mathbf{x}(t)$ for R signals and to $\mathbf{x}_d(t)$ for QR signals. For standard WL receivers ($M = 2$), $\mathbf{x}_M(t)$ corresponds to $\widetilde{\mathbf{x}}(t)$ for R signals and to $\widetilde{\mathbf{x}}_d(t)$ for QR signals. We then deduce from (1) and (4) to (6), that $\mathbf{x}_M(t)$ always takes the form

$$\mathbf{x}_M(t) = \sum_{\ell} b_\ell \mathbf{g}_M(t-\ell T) + \sum_{1\le p\le P}\sum_{\ell} b_{p,\ell}\mathbf{g}_{p,M}(t-\ell T) + \boldsymbol{\epsilon}_M(t)$$

$$= \sum_{\ell} \mathbf{G}_M(t-\ell T)\mathbf{b}_\ell + \boldsymbol{\epsilon}_M(t)$$
$$\stackrel{\text{def}}{=} \sum_{\ell} b_\ell \mathbf{g}_M(t-\ell T) + \mathbf{n}_M(t). \quad (7)$$

Here, $\mathbf{g}_M(t)$, $\mathbf{g}_{p,M}(t)$, $\boldsymbol{\epsilon}_M(t)$ and $\mathbf{n}_M(t)$ are defined in a similar way as $\mathbf{x}_M(t)$, where $\mathbf{x}(t)$ is replaced by $\mathbf{g}(t)$, $\mathbf{g}_p(t)$, $\boldsymbol{\epsilon}(t)$ and $\mathbf{n}(t)$, respectively, whereas $\mathbf{G}_1(f) = \mathbf{G}(f)$ for R signals and $\mathbf{G}_1(f) = \mathbf{G}_d(f)$ for QR signals, $\mathbf{G}_2(f) = \widetilde{\mathbf{G}}(f)$ for R signals and $\mathbf{G}_2(f) = \widetilde{\mathbf{G}}_d(f)$ for QR signals.

III. Linear and two-input WL MMSE receivers

A. L and two-input WL MMSE receivers without any structure constraint

A generic M-input MMSE receiver having no structure constraint corresponds to a continuous-time (CT) receiver, $\mathbf{w}_M^*(-t)$, of dimension $N \times 1$ (for $M = 1$) and $2N \times 1$ (for $M = 2$), whose output, $y_M(t) = \mathbf{w}_M^*(-t) \otimes \mathbf{x}_M(t)$, minimizes, at each time sample nT, the MSE criterion, MSE $= \mathrm{E}(|b_n - y_M(nT)|^2)$.

If the SO cyclostationarity of the MUI is exploited in the MSE criterion minimization, the associated M-input MMSE receiver, which then becomes optimal, is denoted by $\mathbf{w}_{M_o}^*(-t)$, called (o) in the following, and its frequency response, $\mathbf{w}_{M_o}^*(f)$, has been proved in [2] to be defined by

$$\mathbf{w}_{M_o}(f) = \mathbf{G}_M(f)[(N_0/\pi_b)\mathbf{I}_{P+1} + 1/T \sum_{\ell} \mathbf{G}_M^H(f-\ell/T)\mathbf{G}_M(f-\ell/T)]^{-1}\mathbf{f}$$
$$\stackrel{\text{def}}{=} \mathbf{G}_M(f)\mathbf{C}_{M_o}^d(f)\mathbf{f} \stackrel{\text{def}}{=} \mathbf{G}_M(f)\mathbf{c}_{M_o}^d(f). \quad (8)$$

Here $\pi_b \stackrel{\text{def}}{=} \mathrm{E}(b_k^2)$, N_0 is the power spectral density of each component of the noise vector $\boldsymbol{\epsilon}(t)$, $\mathbf{f}$ is the $(P+1)\times 1$ vector defined by $\mathbf{f} = [1, 0, ..., 0]^T$, $\mathbf{C}_{M_o}^d(f)$ is the $(P+1)\times(P+1)$ inverse matrix appearing in (8), which is periodic of period $1/T$, whereas $\mathbf{c}_{M_o}^d(f) \stackrel{\text{def}}{=} \mathbf{C}_{M_o}^d(f)\mathbf{f}$ is a $(P+1)\times 1$ vector. Note that the implementation of the receivers (8) requires the a priori knowledge or estimation of N_0 and $\mathbf{G}(t)$, and then of $\mathbf{H}(t)$, i.e., of the impulse response of both the SOI and MUI channel vectors, which may be cumbersome for a practical implementation.

If the SO cyclostationarity of the MUI is not exploited in the MSE criterion minimization, by falsely assuming stationary MUI, the associated M-input MMSE receiver is denoted by $\mathbf{w}_{M_s}^*(-t)$, called (s) in the following, and its frequency response, $\mathbf{w}_{M_s}^*(f)$, has been proved in [2] to be defined by

$$\mathbf{w}_{M_s}(f) = \Big\{(1/\pi_b) + (1/T)\sum_{\ell} \mathbf{g}_M^H(f-\ell/T)$$
$$[\mathbf{R}_{n,M}^0(f-\ell/T)]^{-1}\mathbf{g}_M(f-\ell/T)\Big\}^{-1}[\mathbf{R}_{n_M}^0(f)]^{-1}\mathbf{g}_M(f)$$
$$\stackrel{\text{def}}{=} c_{M_s}^d(f)[\mathbf{R}_{n_M}^0(f)]^{-1}\mathbf{g}_M(f). \quad (9)$$

Here, $c_{M_s}^d(f)$ is the inverse scalar term appearing in (9), which is periodic of period $1/T$, $\mathbf{g}_1(f) = \mathbf{g}(f)$ for R signals and $\mathbf{g}_1(f) = \mathbf{g}_d(f)$ for QR signals, $\mathbf{g}_2(f) = \widetilde{\mathbf{g}}(f)$ for R signals and $\mathbf{g}_2(f) = \widetilde{\mathbf{g}}_d(f)$ for QR signals, $\mathbf{R}_{n,M}^0(f)$ defined as the Fourier transform of $\mathbf{R}_{n,M}^0(\tau) \stackrel{\text{def}}{=} < \mathrm{E}[\mathbf{n}_M(t+\tau/2)\mathbf{n}_M^H(t-\tau/2)] >$ corresponds to the power spectral density matrix of $\mathbf{n}_M(t)$ and is given by:

$$\mathbf{R}_{n,M}^0(f) = \frac{\pi_b}{T}\sum_{p=1}^{P}\mathbf{g}_{p,M}(f)\mathbf{g}_{p,M}^H(f) + N_0\mathbf{I}_{NM}$$
$$= \mathbf{R}_{x,M}^0(f) - \frac{\pi_b}{T}\mathbf{g}_M(f)\mathbf{g}_M^H(f), \quad (10)$$

where $\mathbf{g}_{p,M}(f)$ is defined in a similar way as $\mathbf{g}_M(f)$ but where $\mathbf{g}(f)$ is replaced by $\mathbf{g}_p(f)$ and where $\mathbf{R}_{x,M}^0(f)$ is the power spectral density matrix of $\mathbf{x}_M(t)$, defined in a similar way as $\mathbf{R}_{n,M}^0(f)$, with $\mathbf{x}_M(t)$ instead of $\mathbf{n}_M(t)$. Note that the implementation of the receivers (9) requires the a priori knowledge or estimation of $\mathbf{R}_n^0(f)$ and $\mathbf{g}(t)$, and then of $\mathbf{h}(t)$, i.e., of the impulse response of the SOI channel vector only, discarding the need to estimate the MUI channel vectors, which may be advantageous for a practical implementation.

B. L and two-input WL MMSE receivers with a particular structure constraint

Most of L and WL MMSE receivers of the literature are implemented at the symbol rate, after a matched filtering operation to the pulse shaping filter, and have thus a particular structure constraint. To compute these MMSE receivers, we denote by $\mathbf{x}_v(t) \stackrel{\text{def}}{=} v^*(-t) \otimes \mathbf{x}(t)$, and $\mathbf{x}_{v,M}(t)$ the observation vector and the M-input observation vector respectively, after matched filtering operation to the pulse-shaping filter. Note that $\mathbf{x}_{v,M}(t)$ is defined in a similar way as $\mathbf{x}_M(t)$ but where $\mathbf{x}(t)$ is replaced by $\mathbf{x}_v(t)$. Denoting by ${\mathbf{w}_{M_{sc}}^d}^*(-kT)$, the M-input discrete time (DT) receiver whose output at time nT, $y_M(nT) = \sum_k {\mathbf{w}_{M_{sc}}^d}^H(-kT)\mathbf{x}_{v,M}((n-k)T))$, minimizes the MSE, it has been proved in [2] that the frequency response, ${\mathbf{w}_{M_{sc}}^d}^*(f)$, of this receiver, called (sc) in the following, is such that

$$\mathbf{w}_{M_{sc}}^d(f) = \pi_b[\mathbf{R}_{x_{v,M}}^d(f)]^{-1}\mathbf{g}_{v,M}^d(f) \quad (11)$$

if $v(f)$ does not vanish in $[-1/2T, +1/2T]$. Otherwise $\mathbf{w}_{M_{sc}}^d(f) = \mathbf{0}$ for the frequencies f which are outside the support of $\mathbf{g}_{v,M}^d(f)$, i.e., such that $\mathbf{x}_{v,M}^d(f) = \mathbf{0}$, where $\mathbf{x}_{v,M}^d(f)$ is the Fourier transform of $\mathbf{x}_{v,M}(nT)$. Here, $\mathbf{g}_{v,M}^d(f)$ is the frequency response of the DT SOI channel vector $\mathbf{g}_{v,M}(kT)$, where $\mathbf{g}_{v,M}(t)$ is defined in a similar way as $\mathbf{x}_M(t)$ but where $\mathbf{x}(t)$ is replaced by $\mathbf{g}_v(t) \stackrel{\text{def}}{=} v^*(-t) \otimes \mathbf{g}(t)$, whereas $\mathbf{R}_{x_{v,M}}^d(f)$ is the Fourier transform of matrix $\mathbf{R}_{x_{v,M}}^d(kT) \stackrel{\text{def}}{=} \mathrm{E}[\mathbf{x}_{v,M}(nT)\mathbf{x}_{v,M}^H((n-k)T)]$. Note that the implementation of the receivers (11) requires the a priori knowledge or estimation of $\mathbf{R}_{x_{v,M}}^d(f)$ and $\mathbf{g}_{v,M}^d(f)$ and then of $\mathbf{h}(kT)$, i.e., of the DT impulse response of the

SOI channel vector only.

C. Generic output of the linear and two-input WL MMSE receivers before decision

It has been deduced in [2] from (8), (9) and (11) that the generic output of the L and WL receivers considered in [2] can be written as

$$y_{M_g}(k) = \int \mathbf{w}_{M_g}^H(f)\mathbf{x}_{M_g}(f)e^{j2\pi fkT}df \qquad (12)$$

where

$$\begin{aligned}(y_{M_g}(k), \mathbf{w}_{M_g}(f), \mathbf{x}_{M_g}(f)) &= (y_{M_o}(k), \mathbf{w}_{M_o}(f), \mathbf{x}_M(f)) \\ &= (y_{M_s}(k), \mathbf{w}_{M_s}(f), \mathbf{x}_M(f)) \\ &= (y_{M_{sc}}(k), \mathbf{w}_{M_{sc}}^d(f), \mathbf{x}_{v_M}(f))\end{aligned}$$

for the (o), (s) and (sc) receivers, respectively.

IV. Three-input (s) WL MMSE receivers

We explain, in this section, why the suboptimality of the (s) two-input WL MMSE receiver in the presence of MUI is more pronounced for QR signals and increases with the bandwidth for both R and QR signals. Then, we propose a (s) three-input WL MMSE receiver, which is shown to be quasi-optimal in most cases, and whose implementation does not require the MUI channel knowledge, hence its practical interest.

A. Sub-optimality of (s) two-input WL MMSE receivers

It has been recalled in [2] that, for both R and QR data-like MUI, the total noise $\mathbf{n}(t)$ has both non-conjugate and conjugate SO cyclostationarity. More precisely, under the previous assumptions, it is easy to verify that the two correlation matrices, $\mathbf{R}_n(t,\tau) \stackrel{\text{def}}{=} \mathrm{E}[\mathbf{n}(t+\tau/2)\mathbf{n}^H(t-\tau/2)]$ and $\mathbf{C}_n(t,\tau) \stackrel{\text{def}}{=} \mathrm{E}[\mathbf{n}(t+\tau/2)\mathbf{n}^T(t-\tau/2)]$, of $\mathbf{n}(t)$ are periodic functions of t, whose periods are equal to T and T, respectively for R signals, and to T and $2T$, respectively for QR signals. These two matrices have then Fourier series expansions, generating the so-called non-conjugate, α_i and conjugate, β_i, $i \in \mathbb{Z}$, SO cyclic frequencies respectively of observations [2]. For R signals, $\alpha_i = \beta_i = i/T$, whereas for QR signals, $\alpha_i = i/T$ and $\beta_i = (2i+1)/2T$ [19]–[21]. Note that the different behavior of the (s) two-input WL MMSE receiver for R and QR signals is mainly directly related to the different conjugate SO cyclostationarity properties of the latter. Indeed, for R signals, the (s) two-input WL MMSE receiver only exploits the information contained at the zero non-conjugate and conjugate, $(\alpha,\beta) = (0,0)$, SO cyclic frequencies of $\mathbf{x}(t)$ through the exploitation of the temporal mean of the first correlation matrix, $\mathbf{R}_{\tilde{x}}(t,\tau) \stackrel{\text{def}}{=} \mathrm{E}[\widetilde{\mathbf{x}}(t+\tau/2)\widetilde{\mathbf{x}}^H(t-\tau/2)]$. For QR signals, the derotation operation does not modify the non-conjugate cyclic frequencies but translates the conjugate cyclic frequencies of $-1/2T$. The non-conjugate and conjugate SO cyclic frequencies of $\mathbf{n}_d(t)$ are thus given by $\alpha_{d,i} = \alpha_i = i/T$ and $\beta_{d,i} = \beta_i - 1/2T = i/T$, respectively. In this case, for QR signals, the (s) two-input WL MMSE receiver only exploits the information contained at the zero non-conjugate and conjugate, $(\alpha_{d,0},\beta_{d,0}) = (0,0)$, SO cyclic frequencies of $\mathbf{x}_d(t)$ through the exploitation of the temporal mean of the first correlation matrix, $\mathbf{R}_{\tilde{x}_d}(t,\tau) \stackrel{\text{def}}{=} \mathrm{E}[\widetilde{\mathbf{x}}_d(t+\tau/2)\widetilde{\mathbf{x}}_d^H(t-\tau/2)]$. This is equivalent to exploit the energy contained in $(\alpha_0,\beta_0) = (0,1/2T)$.

However, the main SO cyclic energy of R signals is contained in the SO cyclic frequencies $(\alpha_0,\beta_0) = (0,0)$, whatever the real-valued filter $v(t)$, whereas the SO cyclic energy contained in $\alpha_i = \beta_i = i/T, i \neq 0$, increases with the signal bandwidth, hence the quasi-optimality of the (s) two-input WL MMSE for small bandwidth and the suboptimality of the latter as the bandwidth increases. On the contrary, the main SO cyclic energy of QR signals is contained in the SO cyclic frequencies $(\alpha_0,\beta_0,\beta_{-1}), = (0,1/2T,-1/2T)$, whatever the real-valued filter $v(t)$, with a similar cyclic energy on β_0 and β_{-1}. Besides, the SO cyclic energy contained in $\alpha_i = i/T$, $i \neq 0$, and $\beta_i = (2i+1)/2T$, $i \neq 0$ and $i \neq -1$, increases with the signal bandwidth. As a consequence, the (s) two-input WL MMSE receiver only exploit half of the main conjugate SO cyclic information, and is thus suboptimal for QR signals whatever the bandwidth, even small, whereas its sub-optimality increases with the bandwidth.

B. Three-input FRESH model

To overcome, for both R and QR signals, the limitations of the (s) two-input WL MMSE receiver, it is necessary to implement, in both cases, a WL MMSE receiver which is able to take full account of more SO cyclic energy than the (s) two-input receiver. To optimize a compromise between performance and complexity, we limit the analysis to three-input receivers instead of two-input ones. Such a receiver can be obtained, for R and QR signals, by implementing the (s) WL MMSE receiver from the three-input FRESH model defined, for R signals, by

$$\mathbf{x}_3(t) \stackrel{\text{def}}{=} [\mathbf{x}^T(t), \mathbf{x}^H(t), e^{-j2\pi t/T}\mathbf{x}^H(t)]^T \qquad (13)$$

and for QR signals, by

$$\begin{aligned}\mathbf{x}_3(t) &\stackrel{\text{def}}{=} [\mathbf{x}_d^T(t), \mathbf{x}_d^H(t), e^{-j2\pi t/T}\mathbf{x}_d^H(t)]^T \\ &= j^{-t/T}[\mathbf{x}^T(t), e^{j2\pi t/2T}\mathbf{x}^H(t), e^{-j2\pi t/2T}\mathbf{x}^H(t)]^T \\ &\stackrel{\text{def}}{=} j^{-t/T}\mathbf{x}_3'(t). \qquad (14)\end{aligned}$$

In both cases, using (1), $\mathbf{x}_3(t)$ can be written as

$$\mathbf{x}_3(t) = \sum_\ell b_\ell \mathbf{g}_3(t-\ell T) + \sum_{1\leq p\leq P}\sum_\ell b_{p,\ell}\mathbf{g}_{p,3}(t-\ell T) + \boldsymbol{\epsilon}_3(t)$$

$$= \sum_{\ell} \mathbf{G}_3(t-\ell T)\mathbf{b}_\ell + \boldsymbol{\epsilon}_3(t)$$
$$\stackrel{\text{def}}{=} \sum_{\ell} b_\ell \mathbf{g}_3(t-\ell T) + \mathbf{n}_3(t). \quad (15)$$

Here, $\boldsymbol{\epsilon}_3(t)$ and $\mathbf{n}_3(t)$ correspond to $\mathbf{x}_3(t)$ with $\boldsymbol{\epsilon}(t)$ and $\mathbf{n}(t)$, respectively, instead of $\mathbf{x}(t)$ for both R and QR signals, whereas $\mathbf{g}_3(t) \stackrel{\text{def}}{=} [\mathbf{g}^T(t), \mathbf{g}^H(t), e^{-j2\pi t/T}\mathbf{g}^H(t)]^T$ for R signals and $\mathbf{g}_3(t) \stackrel{\text{def}}{=} [\mathbf{g}_d^T(t), \mathbf{g}_d^H(t), e^{-j2\pi t/T}\mathbf{g}_d^H(t)]^T$ for QR signals. The vector $\mathbf{g}_{p,3}(t)$ is defined in a similar way as $\mathbf{g}_3(t)$ but where $\mathbf{g}_p(t)$ replaces $\mathbf{g}(t)$, whereas matrix $\mathbf{G}_3(t)$ is defined by $\mathbf{G}_3(t) \stackrel{\text{def}}{=} [\mathbf{g}_3(t), \mathbf{g}_{1,3}(t), .., \mathbf{g}_{P,3}(t)]$. Note that, for R signals, the three-input model might also be defined by $\mathbf{x}_3(t) \stackrel{\text{def}}{=} [\mathbf{x}^T(t), \mathbf{x}^H(t), e^{j2\pi t/T}\mathbf{x}^H(t)]^T$. For QR signals, the three-input model $\mathbf{x}_3'(t)$ might have also been chosen instead of $\mathbf{x}_3(t)$, which has been done in [15]. An alternative three-input model for QR signals might also be defined by $\mathbf{x}_3(t) \stackrel{\text{def}}{=} [\mathbf{x}_d^T(t), \mathbf{x}_d^H(t), e^{j2\pi t/T}\mathbf{x}_d^H(t)]^T$ provided that $\mathbf{x}_d(t)$ is, in this case, defined by $\mathbf{x}_d(t) \stackrel{\text{def}}{=} j^{t/T}\mathbf{x}(t)$.

It is straightforward to verify that the temporal mean of the first correlation matrix, $\mathbf{R}_{x_3}(t,\tau) \stackrel{\text{def}}{=} \mathrm{E}[\mathbf{x}_3(t+\tau/2)\mathbf{x}_3^H(t-\tau/2)]$ of $\mathbf{x}_3(t)$, exploits the information contained in $(\alpha_0, \alpha_{-1}, \alpha_1, \beta_0, \beta_{-1}) = (0, -1/T, 1/T, 0, -1/T)$ for R signals, and in $(\alpha_0, \alpha_{-1}, \alpha_1, \beta_{d,0}, \beta_{d,-1}) = (0, -1/T, 1/T, 0, -1/T)$ for QR signals, which corresponds, in this latter case, to $(\alpha_0, \alpha_{-1}, \alpha_1, \beta_0, \beta_{-1}) = (0, -1/T, 1/T, 1/2T, -1/2T)$. This allows us to exploit the main non-conjugate and conjugate SO cyclic frequencies of R and QR signals whatever the pulse shaping filter. Note that a TI linear processing of $\mathbf{x}_3(t)$ becomes now a time variant (TV) WL processing of $\mathbf{x}(t)$, called here three-input WL FRESH processing of $\mathbf{x}(t)$.

C. The (s) three-input WL MMSE receiver

To compute, for R and QR signals, the (s) three-input WL MMSE receiver, we assume that the total noise, $\mathbf{n}_3(t)$, appearing in (15) is falsely SO stationary. We denote by $\mathbf{w}_{3_s}^*(-t)$ the associated 3-input WL MMSE receiver, whose output, $y_{3_s}(t) = \mathbf{w}_{3_s}^H(-t) \otimes \mathbf{x}_3(t)$ minimizes, at each time sample nT, the MSE criterion, $\mathrm{MSE} = \mathrm{E}(|b_n - y_{3_s}(nT)|^2)$. Under these assumptions, using a method similar to that used in [2] to compute the (s) two-input WL MMSE receiver, it is straightforward to prove that the frequency response, $\mathbf{w}_{3_s}^*(f)$, of this receiver is such that

$$\mathbf{w}_{3_s}(f) = \Big\{(1/\pi_b) + (1/T)\sum_{\ell} \mathbf{g}_3^H(f-\ell/T) [\mathbf{R}_{n_3}^0(f-\ell/T)]^{-1}\mathbf{g}_3(f-\ell/T)\Big\}^{-1} [\mathbf{R}_{n_3}^0(f)]^{-1}\mathbf{g}_3(f)$$
$$\stackrel{\text{def}}{=} c_{3_s}^d(f)[\mathbf{R}_{n_3}^0(f)]^{-1}\mathbf{g}_3(f). \quad (16)$$

Here, $c_{3_s}^d(f)$ is the inverse scalar term appearing in (16), which is periodic of period $1/T$, whereas $\mathbf{R}_{n_3}^0(f)$, defined as the Fourier transform of $\mathbf{R}_{n_3}^0(\tau) \stackrel{\text{def}}{=} < \mathrm{E}[\mathbf{n}_3(t+\tau/2)\mathbf{n}_3^H(t-\tau/2)] >$, corresponds to the power spectral density matrix of $\mathbf{n}_3(t)$. Using (15), it is easy to verify that $\mathbf{R}_{n_3}^0(f)$ is given by

$$\mathbf{R}_{n_3}^0(f) = \mathbf{R}_{x_3}^0(f) - \frac{\pi_b}{T}\mathbf{g}_3(f)\mathbf{g}_3^H(f), \quad (17)$$

where $\mathbf{R}_{x_3}^0(f)$ is the power spectral density matrix of $\mathbf{x}_3(t)$, defined in a similar way as $\mathbf{R}_{n_3}^0(f)$, with $\mathbf{x}_3(t)$ instead of $\mathbf{n}_3(t)$. The output, at time kT, of the associated receiver as depicted in Fig. 1, is given by

$$y_{3_s}(k) = \int \mathbf{w}_{3_s}^H(f)\mathbf{x}_3(f)e^{j2\pi fkT}df$$
$$= \int c_{3_s}^d(f)\mathbf{g}_3^H(f)[\mathbf{R}_{n_3}^0(f)]^{-1}\mathbf{x}_3(f)e^{j2\pi fkT}df. \quad (18)$$

Note that the implementation of the receivers (16) requires the a priori knowledge or estimation of $\mathbf{R}_{n_3}^0(f)$ and $\mathbf{g}_3(f)$, and then of $\mathbf{h}(t)$, i.e., of the impulse response of the SOI channel vector only, discarding the need to estimate the MUI channel vectors, which may be advantageous for a practical implementation.

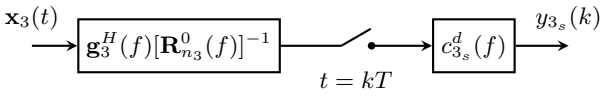

Fig. 1. Structure of the three-input WL MMSE receiver

Furthermore, it is important to note, which is proved in Appendix A, that, for both R and QR signals, the optimal three-input WL MMSE receiver whose input is $\mathbf{x}_3(t)$, is the receiver whose frequency response, $\mathbf{w}_{3_o}^*(f)$, is given by $\mathbf{w}_{3_o}^*(f) = [\mathbf{w}_{2_o}^H(f), \mathbf{0}^T]^T$, where $\mathbf{w}_{2_o}(f)$ is given by (8) for $M = 2$. This confirms that the optimal two-input WL MMSE receiver optimally exploits all the SO cyclostationarity of the MUI.

D. SINR at the output of the (s) three-input WL MMSE receiver

D1) *Output of the (s) three-input WL MMSE receiver:* Inserting the Fourier transform $\mathbf{x}_3(f)$ of $\mathbf{x}_3(t)$ given by (15) in (18), we obtain

$$y_{3_s}(k) = b_k \int \mathbf{w}_{3_s}^H(f)\mathbf{g}_3(f)df + \sum_{\ell\neq k} b_\ell \int \mathbf{w}_{3_s}^H(f)\mathbf{g}_3(f)e^{j2\pi f(k-\ell)T}df + \int \mathbf{w}_{3_s}^H(f)\mathbf{n}_3(f)e^{j2\pi fkT}df$$
$$\stackrel{\text{def}}{=} b_k u_{3_{s,0}} + e_{3_s}(k), \quad (19)$$

where it is easy to verify from (16) and (19), that $u_{3_{s,0}}$ is positive real-valued and where $e_{3_s}(k)$ is the contribution of the inter-Symbol Interference (ISI), the MUI and the

background noise in $y_{3_s}(k)$. As b_k are real-valued, it is well-known that, assuming $e_{3_s}(k)$ circular Gaussian distributed, a conventional ML receiver whose input is (19) decides the symbols from the real-part $z_{3_s}(k)$ of $y_{3_s}(k)$ given by

$$z_{3_s}(k) \stackrel{\text{def}}{=} \text{Re}(y_{3_s}(k)) = b_k u_{3_{s,0}} + \text{Re}(e_{3_s}(k)). \quad (20)$$

D2) *SINR at the output of the (s) three-input WL MMSE receiver before decision:* The SER at the output of the (s) three-input WL MMSE receiver $\mathbf{w}_{3_s}^H(f)$ is directly linked to the SINR in $z_{3_s}(k)$, denoted by $\text{SINR}_{3_s}(k)$. Using the property that the quantities $b_k u_{3_{s,0}}$ and $\text{Re}(e_{3_s}(k))$ are uncorrelated, we deduce that $\text{SINR}_{3_s}(k)$ can be written as

$$\begin{aligned}\text{SINR}_{3_s}(k) &= \frac{\pi_b u_{3_{s,0}}^2}{\text{E}[(\text{Re}(e_{3_s}(k)))^2]} \\ &= \frac{2\pi_b u_{3_{s,0}}^2}{\text{E}[|y_{3_s}^2(k)|] + \text{Re}(\text{E}[y_{3_s}^2(k)]) - 2\pi_b u_{3_{s,0}}^2}. \quad (21)\end{aligned}$$

In the presence of R or QR MUI, the CT output $y_{3_s}(t)$ is SO cyclostationary, which implies that $\text{E}[|y_{3_s}^2(k)|]$ and $\text{E}[y_{3_s}^2(k)]$ have Fourier series expansions given by

$$\text{E}[|y_{3_s}^2(k)|] = \sum_{\gamma_i} e^{j2\pi\gamma_i kT} \int r_{y_{3_s}}^{\gamma_i}(f)df \quad (22)$$

$$\text{E}[y_{3_s}^2(k)] = \sum_{\delta_i} e^{j2\pi\delta_i kT} \int c_{y_{3_s}}^{\delta_i}(f)df. \quad (23)$$

Here, the quantities γ_i and δ_i denote the non-conjugate and conjugate SO cyclic frequencies of $y_{3_s}(t)$, respectively, whereas $r_{y_{3_s}}^{\gamma_i}(f)$ and $c_{y_{3_s}}^{\delta_i}(f)$ are the Fourier transforms of the first, $r_{y_{3_s}}^{\gamma_i}(\tau)$, and second, $c_{y_{3_s}}^{\delta_i}(\tau)$, cyclic correlation functions of $y_{3_s}(t)$ for the delay τ and the cyclic frequencies γ_i and δ_i, respectively. Moreover, as $y_{3_s}(t)$ is the output of the TI filter, whose frequency response is $\mathbf{w}_{3_s}^H(f)$ and whose input is $\mathbf{x}_3(t)$, we can write

$$r_{y_{3_s}}^{\gamma_i}(f) = \mathbf{w}_{3_s}^H(f+\gamma_i/2)\mathbf{R}_{x_3}^{\gamma_i}(f)\mathbf{w}_{3_s}(f-\gamma_i/2) \quad (24)$$

$$c_{y_{3_s}}^{\delta_i}(f) = \mathbf{w}_{3_s}^H(f+\delta_i/2)\mathbf{C}_{x_3}^{\delta_i}(f)\mathbf{w}_{3_s}^*(\delta_i/2-f), \quad (25)$$

where $\mathbf{R}_{x_3}^{\gamma_i}(f)$ and $\mathbf{C}_{x_3}^{\delta_i}(f)$ are the Fourier transforms of the first, $\mathbf{R}_{x_3}^{\gamma_i}(\tau)$, and second, $\mathbf{C}_{x_3}^{\delta_i}(\tau)$, cyclic correlation matrices of $\mathbf{x}_3(t)$ for the delay τ and the cyclic frequency γ_i and δ_i respectively. In the presence of data-like MUI, it is straightforward to verify that for both R and QR signals, $\gamma_i = \delta_i = \alpha_i = \beta_{d,i} = i/T$, $i \in \mathbb{Z}$.

This implies that (22) and (23) and then, $\text{SINR}_{3_s}(k)$ do not depend on k and the latter is simply denoted by SINR_{3_s}. Using (22) to (25) into (21), we finally obtain

$$\text{SINR}_{3_s} = \frac{2\pi_b[\int \mathbf{w}_{3_s}^H(f)\mathbf{g}_3(f)df]^2}{\left\{\begin{array}{l}\sum_{\alpha_i}\int[\mathbf{w}_{3_s}^H(f+\alpha_i/2)\mathbf{R}_{x_3}^{\alpha_i}(f)\mathbf{w}_{3_s}(f-\alpha_i/2) \\ +\text{Re}(\mathbf{w}_{3_s}^H(f+\alpha_i/2)\mathbf{C}_{x_3}^{\alpha_i}(f)\mathbf{w}_{3_s}^*(\alpha_i/2-f))]df \\ -2\pi_b[\int \mathbf{w}_{3_s}^H(f)\mathbf{g}_3(f)df]^2\end{array}\right.}, \quad (26)$$

where $\mathbf{g}_3(f) \stackrel{\text{def}}{=} [\mathbf{g}^T(f), \mathbf{g}^H(-f), \mathbf{g}^H(-1/T-f)]^T$ for R signals, whereas $\mathbf{g}_3(f) \stackrel{\text{def}}{=} [\mathbf{g}_d^T(f), \mathbf{g}_d^H(-f), \mathbf{g}_d^H(-1/T-f)]^T = [\mathbf{g}^T(f+1/4T), \mathbf{g}^H(1/4T-f), \mathbf{g}^H(-3/4T-f)]^T$ for QR signals.

V. SINR ANALYSIS FOR ONE MUI

A. Total noise model and statistics

We assume in this section that the total noise $\mathbf{n}(t)$ is composed of a background noise and one data-like MUI, which generates the observation model (1) with $P = 1$. In this context, the purpose of this section is to compute, for R and QR signals, the SINR at the output of the (s) three-input WL MMSE receivers and to compare the latter with those of the two-input MMSE receivers (8), (9) and (11) computed in [2]. Under these assumptions, following a similar approach as in [15], it is straightforward to prove that, for R and QR signals, the matrices $\mathbf{R}_{x_3}^{\alpha_i}(f)$ and $\mathbf{C}_{x_3}^{\alpha_i}(f)$, appearing in (26), can be written as

$$\begin{aligned}\mathbf{R}_{x_3}^{\alpha_i}(f) &= \frac{\pi_b}{T}[\mathbf{g}_3(f+\alpha_i/2)\mathbf{g}_3^H(f-\alpha_i/2) \\ &+ \mathbf{g}_{1,3}(f+\alpha_i/2)\mathbf{g}_{1,3}^H(f-\alpha_i/2)] \\ &+ \mathbf{R}_{\epsilon_3}^{\alpha_i}(f) \quad (27) \\ \mathbf{C}_{x_3}^{\alpha_i}(f) &= \frac{\pi_b}{T}[\mathbf{g}_3(f+\alpha_i/2)\mathbf{g}_3^T(\alpha_i/2-f) \\ &+ \mathbf{g}_{1,3}(f+\alpha_i/2)\mathbf{g}_{1,3}^T(\alpha_i/2-f)] \\ &+ \mathbf{C}_{\epsilon_3}^{\alpha_i}(f). \quad (28)\end{aligned}$$

Here, $\mathbf{g}_{1,3}(f) \stackrel{\text{def}}{=} [\mathbf{g}_1^T(f), \mathbf{g}_1^H(-f), \mathbf{g}_1^H(-1/T-f)]^T$ for R signals, whereas $\mathbf{g}_{1,3}(f) \stackrel{\text{def}}{=} [\mathbf{g}_{1,d}^T(f), \mathbf{g}_{1,d}^H(-f), \mathbf{g}_{1,d}^H(-1/T-f)]^T = [\mathbf{g}_1^T(f+1/4T), \mathbf{g}_1^H(1/4T-f), \mathbf{g}_1^H(-3/4T-f)]^T$ for QR signals. Moreover $\mathbf{R}_{\epsilon_3}^{\alpha_i}(f)$ and $\mathbf{C}_{\epsilon_3}^{\alpha_i}(f)$ are given by

$$\begin{aligned}\mathbf{R}_{\epsilon_3}^{\alpha_i}(f) &= N_0\delta(\alpha_i)\mathbf{I}_{3N} + N_0\delta(\alpha_i+1/T)\mathbf{J}_1^T \\ &+ N_0\delta(\alpha_i-1/T)\mathbf{J}_1 \quad (29) \\ \mathbf{C}_{\epsilon_3}^{\alpha_i}(f) &= N_0\delta(\alpha_i)\mathbf{J}_2 + N_0\delta(\alpha_i+1/T)\mathbf{J}_3, \quad (30)\end{aligned}$$

where N_0 is the power spectral density of each component of the background noise $\boldsymbol{\epsilon}(t)$, whereas $\mathbf{J}_1$, $\mathbf{J}_2$ and $\mathbf{J}_3$ are the $3N \times 3N$ matrices defined by

$$\mathbf{J}_1 = \begin{pmatrix}\mathbf{0} & \mathbf{0} & \mathbf{0} \\ \mathbf{0} & \mathbf{0} & \mathbf{I} \\ \mathbf{0} & \mathbf{0} & \mathbf{0}\end{pmatrix}, \ \mathbf{J}_2 = \begin{pmatrix}\mathbf{0} & \mathbf{I} & \mathbf{0} \\ \mathbf{I} & \mathbf{0} & \mathbf{0} \\ \mathbf{0} & \mathbf{0} & \mathbf{0}\end{pmatrix}, \ \mathbf{J}_3 = \begin{pmatrix}\mathbf{0} & \mathbf{0} & \mathbf{I} \\ \mathbf{0} & \mathbf{0} & \mathbf{0} \\ \mathbf{I} & \mathbf{0} & \mathbf{0}\end{pmatrix}. \quad (31)$$

B. Channels with no delay spread

B1) *Propagation model:* To analyze the comparative behavior of the M-input WL MMSE receivers ($M = 2, 3$), for R and QR signals, in the presence of interference, we assume in this section the presence of one MUI and propagation channels with no delay spread such that

$$\mathbf{h}(t) = \mu\delta(t)\mathbf{h} \ \text{ and } \ \mathbf{h}_1(t) = \mu_1\delta(t-\tau_1)\mathbf{h}_1. \quad (32)$$

Here μ and μ_1 control the amplitude of the SOI and MUI respectively and τ_1 is the delay of the MUI with respect to the SOI. The vectors $\mathbf{h}$ and $\mathbf{h}_1$, random or deterministic, with components $h(i)$ and $h_1(i)$, $i = 1, ..., N$, respectively and such that $\mathrm{E}[|h(i)|^2] = \mathrm{E}[|h_1(i)|^2] = 1$, $i = 1, .., N$, correspond to the channel vectors of the SOI and MUI, respectively. The mean SOI and MUI energy per antenna, E_s and E_1 respectively are given by $E_s = \pi_b \mu^2$ and $E_1 = \pi_{b_1} \mu_1^2$, where $\pi_{b_1} \stackrel{\text{def}}{=} \mathrm{E}(b_{1,k}^2)$. We then denote by ϵ and ϵ_1 the quantities $\epsilon_s \stackrel{\text{def}}{=} E_s\, \mathrm{E}(\|\mathbf{h}\|^2)/N_0 = NE_s/N_0$ and $\epsilon_1 \stackrel{\text{def}}{=} E_1\, \mathrm{E}(\|\mathbf{h}_1\|^2)/N_0 = NE_1/N_0$.

B2) *Deterministic channels and SRRC filters with zero roll-off:* Under the previous assumptions, analytical interpretable expressions of SINR_{3_s} defined by (26) are only possible for a SRRC filter $v(t)$ for the symbol duration T with a zero roll-off ω, i.e., for R, π/2-BPSK and π/2-ASK constellations with $\omega = 0$, which is assumed in this subsection. Otherwise, the computation of SINR_{3_s} can only be done numerically by computer simulations and will be discussed in the following subsections. Moreover, we assume in this subsection deterministic channels and we denote by $\alpha_{s,1} = |\alpha_{s,1}| e^{j\phi_{s,1}} \stackrel{\text{def}}{=} \mathbf{h}^H \mathbf{h}_1 / \|\mathbf{h}\| \|\mathbf{h}_1\|$ the spatial correlation coefficient between the SOI and the MUI, such that $0 \leq |\alpha_{s,1}| \leq 1$. Finally, we denote by $\mathrm{SINR}_{R_{3s}}$ and $\mathrm{SINR}_{QR_{3s}}$ the SINR (26) for R and QR signals, respectively.

After cumbersome derivations, whose some steps are given in Appendix B, it is proved that, for synchronous SOI and MUI ($\tau_1 = 0$), whatever the values of ϵ_s, ϵ_1 and $\alpha_{s,1}$, $\mathrm{SINR}_{R_{3s}} = \mathrm{SINR}_{QR_{3s}}$, showing equivalent performance of the (s) three-input WL MMSE receiver for R and QR signals, which was not the case for the (s) two-input WL MMSE receiver, as shown in [2].

When $|\alpha_{s,1}| \neq 1$, i.e., when there exists a spatial discrimination between the SOI and the MUI (which requires $N > 1$), assuming a strong MUI ($\epsilon_1 \gg 1$), we deduce from the results of Appendix B, the following expressions:

$$\mathrm{SINR}_{R_{3,s}} \approx 2\epsilon_s \left(1 - |\alpha_{s,1}|^2 \left(\frac{(1+8\cos^2\phi_{s,1}) - |\alpha_{s,1}|^2(1+2\cos^2\phi_{s,1})^2}{9 - |\alpha_{s,1}|^2(5+4\cos^2\phi_{s,1})}\right)\right) \quad (33)$$

$$\mathrm{SINR}_{QR_{3,s}} \approx 2\epsilon_s \left(1 - |\alpha_{s,1}|^2 \left(\frac{A(\epsilon_s, |\alpha_{s,1}|^2, \cos^2\psi_{s,1}, \cos^2\zeta_{s,1})}{B(\epsilon_s, |\alpha_{s,1}|^2, \cos^2\psi_{s,1}, \cos^2\zeta_{s,1})}\right)\right) \quad (34)$$

where A and B are second-order polynomial in ϵ_s, whereas $\psi_{s,1} \stackrel{\text{def}}{=} \phi_{s,1} - \pi\tau_1/2T$ and $\zeta_{s,1} \stackrel{\text{def}}{=} \phi_{s,1} + \pi\tau_1/2T$. We deduce from (33) and (34) that $\mathrm{SINR}_{R_{3s}}/\epsilon_s$ does not depend on ϵ_s, while $\mathrm{SINR}_{QR_{3s}}/\epsilon_s$ depends on ϵ_s, which proves the absence (for R signals) and the presence (for QR signals) of ISI in the output $z_{3_s}(k)$. Note that for $\epsilon_s \ll 1$, i.e., when the ISI becomes negligible with respect to the noise in $z_{3_s}(k)$, (34) reduces to

$$\mathrm{SINR}_{QR_{3,s}} \approx 2\epsilon_s \left(1 - |\alpha_{s,1}|^2 \left(\frac{(1-|\alpha_{s,1}|^2)(1+\Gamma)^2 + (2-\Gamma)\Gamma}{(1-|\alpha_{s,1}|^2)(5+2\Gamma) + 2(2-\Gamma)}\right)\right);\ \epsilon_s \ll 1, \quad (35)$$

where $\Gamma \stackrel{\text{def}}{=} \cos^2\psi_{s,1} + \cos^2\zeta_{s,1}$. For synchronous SOI and MUI, $\Gamma = 2\cos^2\phi_{s,1}$ and we verify that (33) and (35) give the same expressions.

Furthermore, when $|\alpha_{s,1}| = 1$, i.e., when there is no spatial discrimination between the SOI and the MUI, which is in particular the case for $N = 1$, assuming $\epsilon_1 \gg 1$, we obtain after cumbersome derivations the following expressions:

$$\mathrm{SINR}_{R_{3,s}} \approx 2\epsilon_s(1 - \cos^2\phi_{s,1}); \quad \phi_{s,1} \neq k\pi \quad (36)$$

$$= \frac{2\epsilon_s}{1 + 2\epsilon_1}; \quad \phi_{s,1} = k\pi \quad (37)$$

whereas (34) reduces to

$$\mathrm{SINR}_{QR_{3,s}} \approx 2\epsilon_s \left(1 - \frac{\cos^2\psi_{s,1} + \cos^2\zeta_{s,1}}{2}\right); \quad (\psi_{s,1}, \zeta_{s,1}) \neq (k_1\pi, k_2\pi) \text{ and } \epsilon_s \ll 1 \quad (38)$$

$$= \frac{2\epsilon_s}{1 + 2\epsilon_1}; (\psi_{s,1}, \zeta_{s,1}) = (k_1\pi, k_2\pi). \quad (39)$$

Again, for synchronous SOI and MUI, $\psi_{s,1} = \zeta_{s,1} = \phi_{s,1}$ and we verify that (38) corresponds to (36). Note that expressions (35) and (38), obtained for $\epsilon_s \ll 1$, correspond to the SINR at the output of the three-input WL pseudo-MLSE receiver obtained in [15, (63) and (64)] for QR signals, which does not take into account the ISI in $z_{3_s}(k)$, which is processed by the Viterbi algorithm. Comparing (36) to [2, (60)], we deduce, for $\epsilon_1 \gg 1$, the following result:

$$\mathrm{SINR}_{R_{3,s}} = \mathrm{SINR}_{R_{2,o}} = \mathrm{SINR}_{R_{2,s}} = \mathrm{SINR}_{R_{2,sc}} \approx 2\epsilon_s(1 - \cos^2\phi_{s,1}); \quad \phi_{s,1} \neq k\pi, \quad (40)$$

while comparing (38) to [2, (62) and (64)], we deduce, for $\epsilon_s \ll 1 \ll \epsilon_1$, that

$$\mathrm{SINR}_{QR_{3,s}} = \mathrm{SINR}_{QR_{2,o}} = \mathrm{SINR}_{QR_{2,sc}} \approx 2\epsilon_s \left(1 - \frac{\cos^2\psi_{s,1} + \cos^2\zeta_{s,1}}{2}\right); (\psi_{s,1}, \zeta_{s,1}) \neq (k_1\pi, k_2\pi) \quad (41)$$

$$\mathrm{SINR}_{QR_{2,s}} \approx 2\epsilon_s \left(1 - \frac{1 + \cos^2\psi_{s,1}}{2}\right). \quad (42)$$

These results show, for SRRC filter with zero roll-off, a strong MUI (for R signals) and a strong MUI and a weak SOI (for QR signals), the optimality of the (s) three-input WL MMSE receiver. However, while it does not improve the performance of the (s) two-input WL MMSE receiver for R signals, since the latter is optimal, it outperforms the performance of the latter for QR signals since $\mathrm{SINR}_{QR_{3,s}} \geq \mathrm{SINR}_{QR_{2,s}}$.

To illustrate the previous results, Figs. 2a and 2b show, for the two-input (o), (s) and the three-input (s) WL MMSE

receivers, the variations of the output SINR as a function of $\phi_{s,1}$ for ϵ_s = 10 dB, ϵ_1 = 20 dB, synchronous ($\tau_1 = 0$) SOI and MUI and $|\alpha_{s,1}| = 1$ ($N = 1$) (a), $|\alpha_{s,1}| = 0.75$ (b). Similarly, in the same scenario, Figs. 3a and 3b show the variations of the output SINR as a function of τ_1 for $\phi_{s,1} = \pi/3$. Figs. 2a and 2b show, for synchronous SOI and MUI, for both R and QR signals and for the three receivers, an increasing output SINR as $\cos^2 \phi_{s,1}$ decreases. Moreover, $\text{SINR}_{QR_{2s}}$ is lower for ϵ_s = 10 dB than for $\epsilon_s \ll 1$, due to ISI. Finally, note for $N = 1$, the equivalent optimal performance of the three receivers, except the (s) two-input receiver for QR signals which is clearly sub-optimal. Note for $N > 1$, the equivalent quasi-optimal performance of the (s) three-input receiver for R and QR signals and the sub-optimal performance of the (s) two-input receiver for QR signals. Fig. 3 clearly shows, for R signals, optimal performance, independent of τ_1, for the three receivers, contrary to QR signals for which output performance depend on τ_1. Note, in this case, quasi-optimal performance of the (s) three-input receiver and sub-optimal performance of the (s) two-input receiver. Note finally, for $\tau_1 \neq 2kT$, $k \in \mathbb{Z}$, lower performance of the optimal receiver for QR signals with respect to R ones, showing again the non equivalence of R and QR signals for optimal WL MMSE receivers.

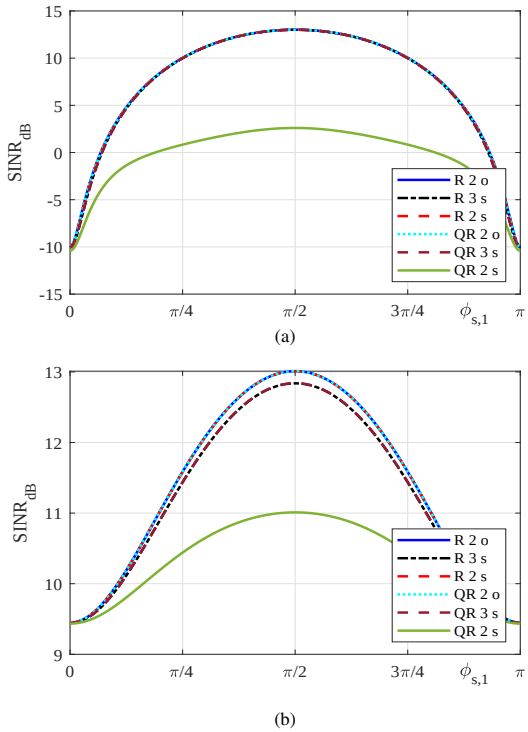

Fig. 2. SINR_R and SINR_{QR} as a function of $\phi_{s,1}$ ($|\alpha_{s,1}| = 1$ (a), $|\alpha_{s,1}| = 0.75$ (b), $\epsilon_s = 10$ dB, $\epsilon_1 = 20$ dB, $\tau_1 = 0$, $\omega = 0$ deterministic channels).

B3) *Deterministic channels and SRRC filter with arbitrary roll-off:* To compare the performance of the (s) three-input

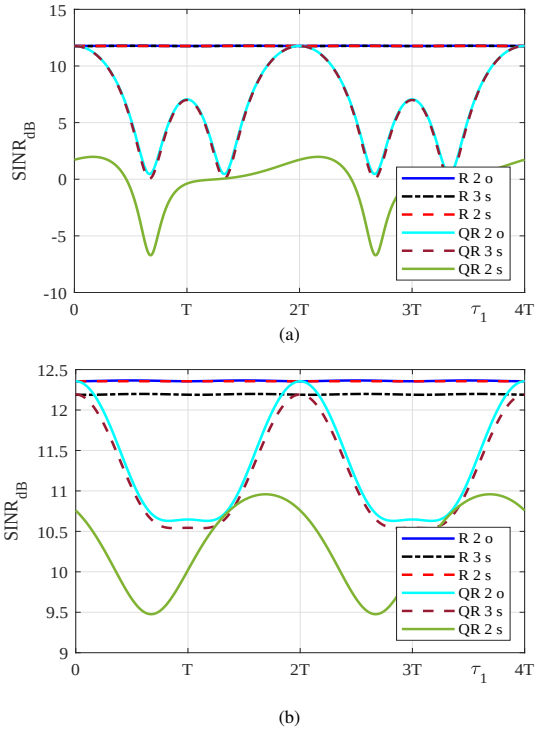

Fig. 3. SINR_R and SINR_{QR} as a function of τ_1 ($|\alpha_{s,1}| = 1$ (a), $|\alpha_{s,1}| = 0.75$ (b), $\epsilon_s = 10$ dB, $\epsilon_1 = 20$ dB, $\phi_{s,1} = \pi/3$, $\omega = 0$ deterministic channels).

WL MMSE receiver to the two-input (o), (s) and (sc) WL MMSE receivers for R and QR signals, $\omega = 0$ and arbitrary values of $\phi_{s,1}$ and τ_1 and also to extend the analysis to arbitrary values of the roll-off ω, we must adopt a statistical perspective. For this purpose, we still consider deterministic channels and we assume that $(\phi_{s,1}, \tau_1)$ are r.v. uniformly distributed on $[0, 2\pi] \times [0, 4T]$. Under these assumptions, choosing $\epsilon_s = 10$ dB and $\epsilon_1 = 20$ dB, Figs. 4 and 5 show, for R and QR signals respectively, for $N = 1$, $M = 2, 3$ and $\omega = 0$ and 1, the variations of $\Pr[(\text{SINR}_{M_g}/2\epsilon_s)\text{dB} \geq x\text{dB}] \overset{\text{def}}{=} P_{M_g}(x)$ as a function of x (dB). Note that the curves appearing in these figures are built from 10^5 Monte-Carlo simulations where the SINR_{M_g} have been computed from the general expressions [2, eq. (37)] and (26). Fig. 4 shows, for R signals, equivalent performance, independent of the roll-off, of the (sc) and (s) two-input WL MMSE receivers, becoming optimal for $\omega = 0$ and whose sub-optimality increases with ω, due to an increasing power on the cyclic frequency $\beta_{d,-1} = -1/T$. On the contrary, Fig. 4 shows increasing performance with the roll-off of the (s) three-input WL MMSE receiver, which is quasi-optimal whatever the roll-off and which always improve the performance of the (s) two-input WL MMSE receiver. Fig. 5 shows, for QR signals, increasing performance with the roll-off of the four WL MMSE receivers. Note the optimality of the (sc) two-input WL MMSE receiver for a zero roll-off and

an increasing sub-optimality of this receiver as the roll-off increases. Note the worst performance of the (s) two-input WL MMSE receiver and the quasi-optimal performance of the (s) three-input WL MMSE receiver, strongly improving the performance of the (s) two-input receiver, whatever the roll-off value.

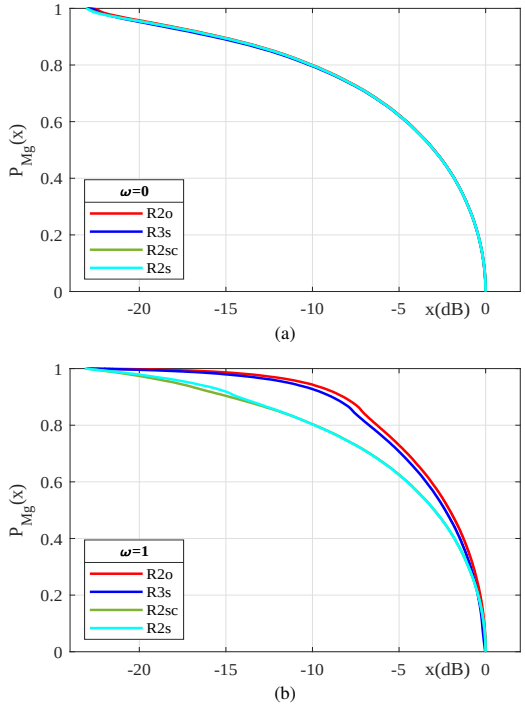

Fig. 4. $P_{M_g}(x)$ as a function of x ($N = 1$, $M = 2, 3$, ϵ_s = 10 dB, ϵ_1 = 20 dB, $\omega = 0$ (a) and 1 (b), deterministic channel, R signals)

B4) *Deterministic channels, and MSK and GMSK signals:* Figs. 6 and 7 show the same variations as Fig. 5, under the same assumptions, but for MSK and GMSK QR signals respectively. We still note, in both cases, the worst performance of the (s) two-input WL MMSE receiver, the sub-optimality of the (sc) two-input WL MMSE receiver and the quasi-optimal performance of the (s) three-input WL MMSE receiver, strongly improving the performance of the (s) two-input receiver. We also note better performance obtained for the MSK signals with respect to GMSK signals due to a greater power on the cyclic frequency $\beta_{d,-1} = -1/T$ [22].

B5) *Rayleigh channels and SRRC filters with arbitrary roll-off:*

To complete the previous results, we consider the assumptions of Figs. 4b and 5b, for R and QR signals respectively. Under these assumptions, Fig. 8 shows, for R and QR signals and for $\omega = 1$, the same variations as Figs. 4b and 5b but for Rayleigh fading channels for which $h(1)$ and $h_1(1)$ are i.i.d zero mean circular Gaussian distributed r.v.. The conclusions of Figs. 4b and 5b hold for Fig. 8a and Fig. 8b with less sub-optimality of (s) and (sc) two-input

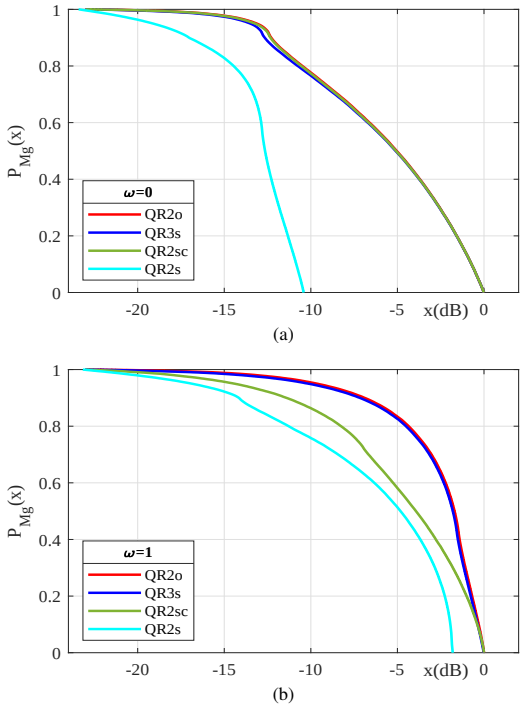

Fig. 5. $P_{M_g}(x)$ as a function of x ($N = 1$, $M = 2, 3$, ϵ_s = 10 dB, ϵ_1 = 20 dB, $\omega = 0$ (a) and 1 (b), deterministic channel, $\pi/2$-ASK QR signals)

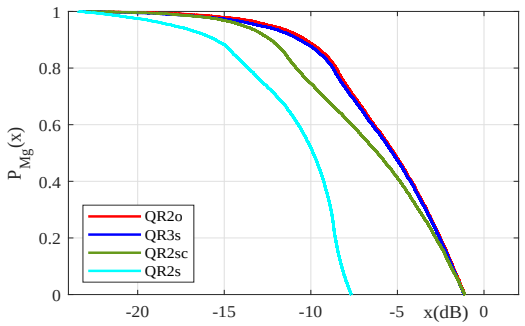

Fig. 6. $P_{M_g}(x)$ as a function of x ($N = 1$, $M = 2, 3$, ϵ_s = 10 dB, ϵ_1 = 20 dB, deterministic channel, MSK signals)

WL MMSE receivers with respect to (s) three-input and (o) two-imput WL MMSE receivers.

C. Two-tap deterministic channels

We consider in this subsection a one-tap deterministic channel for the SOI and a two-tap frequency selective deterministic channel for the MUI such that

$$\begin{aligned} \mathbf{h}(t) &= \mu\delta(t)\mathbf{h} \\ \mathbf{h}_1(t) &= \mu_{1_1}\delta(t-\tau_1)\mathbf{h}_{1_1} + \mu_{1_2}\delta(t-\tau_1-T)\mathbf{h}_{1_2}, \end{aligned} \quad (43)$$

where μ_{1_1} and μ_{1_2} control the amplitudes of the first and second paths of the MUI, whereas $\mathbf{h}_{1_1}$ and $\mathbf{h}_{1_2}$ correspond to the channel vectors of the latter, such that $\|\mathbf{h}_{1_1}\|^2 =$

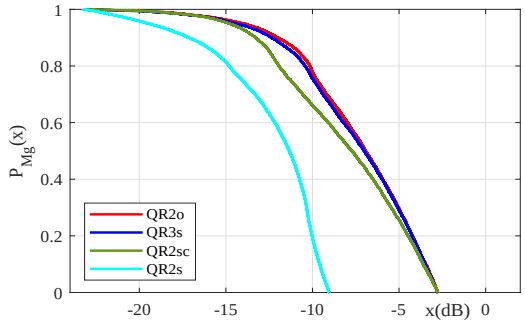

Fig. 7. $P_{M_g}(x)$ as a function of x ($N = 1$, $M = 2, 3$, ϵ_s = 10 dB, ϵ_1 = 20 dB, deterministic channel, GMSK signals)

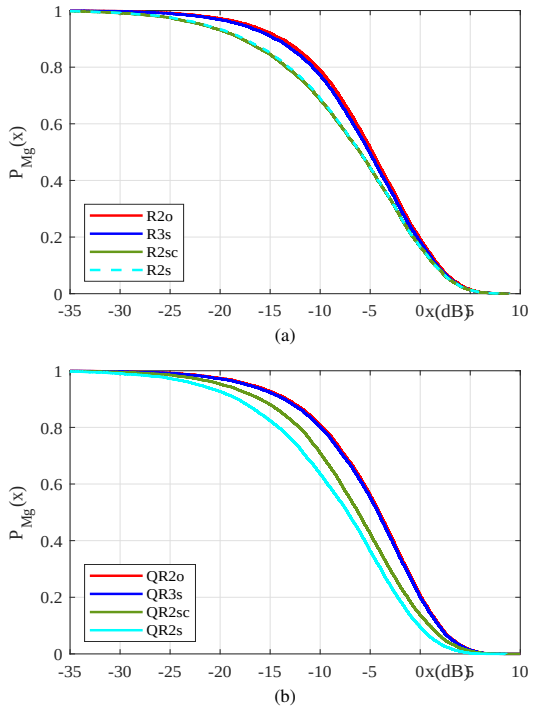

Fig. 8. $P_{M_g}(x)$ as a function of x ($N = 1$, $M = 2, 3$, ϵ_s = 10 dB, ϵ_1 = 20 dB, $\omega = 1$, Rayleigh channel, (a) R and (b) $\pi/2$-ASK QR signals)

$\|\mathbf{h}_{1_2}\|^2 = N$. Under these assumptions and for SRRC pulse shaping filters, it is straightforward to verify that $\pi_1 = (\mu_{1_1}^2 + \mu_{1_2}^2)\pi_{b_1}$. We assume that $(\phi_{s,1_1}, \phi_{s,1_2}, \tau_1)$ are r.v. uniformly distributed on $[0, 2\pi] \times [0, 2\pi] \times [0, 4T]$, where $\phi_{s,1_1}$ and $\phi_{s,1_2}$ are the phases of $\mathbf{h}^H\mathbf{h}_{1_1}$ and $\mathbf{h}^H\mathbf{h}_{1_2}$, respectively. Under these assumptions, Figs. 9a and 9b show, for R and QR signals, respectively and for $\omega = 1$, the same variations as Figs. 4b and 5b for $\mu_{1_1} = \mu_{1_2}$. The conclusions of Figs. 4b and 5b hold for Figs. 9a and 9b.

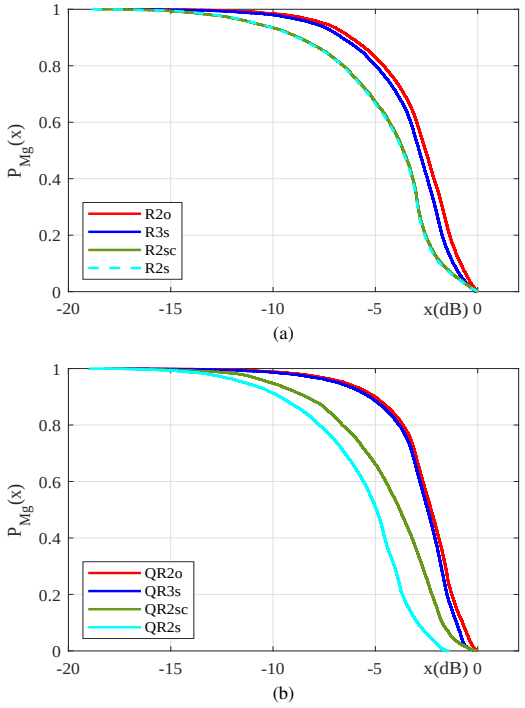

Fig. 9. $P_{M_g}(x)$ as a function of x ($N = 1$, $M = 2, 3$, ϵ_s = 10 dB, ϵ_1 = 20 dB, $\mu_{1_1} = \mu_{1_2}$, $\omega = 1$, deterministic channel, (a) R and (b) $\pi/2$-ASK QR signals)

VI. SER at the output of the WL MMSE receivers for one MUI

We show in this section that the main messages of the previous section, deduced from an output SINR analysis remain valid from an output SER analysis.

A. Theoretical closed-form expressions

To compare the previous M-input ($M = 2, 3$) WL MMSE receivers for R and QR signals from an output SER analysis, we still assume in this section that the total noise $\mathbf{n}(t)$ is composed of a Gaussian distributed background noise $\boldsymbol{\epsilon}(t)$ and a single MUI, which generates the observation model (7) with $P = 1$. From (7) and (15) we get the generic real part, $z_{M_g}(k)$, of the generic output $y_{M_g}(k)$, of the different M-input WL MMSE receivers for $g = o, s, sc$.

$$z_{M_g}(k) = \underbrace{b_k u_{M_{g,0}}}_{\text{SOI}} + \underbrace{\sum_{\ell \neq k} b_\ell u_{M_{g,k-\ell}}}_{\text{ISI}} + \underbrace{\sum_{\ell} b_{1,\ell} u_{M_{1,g,k-\ell}}}_{\text{MUI}} + \underbrace{\epsilon_{M_g}(k)}_{\text{BN}} \quad (44)$$

where $u_{M_{g,k}} \overset{\text{def}}{=} \text{Re}[\int \mathbf{w}_{M_g}^H(f)\mathbf{g}_{M_g}(f)e^{j2\pi fkT}df]$, $u_{M_{1,g,,k}} \overset{\text{def}}{=} \text{Re}[\int \mathbf{w}_{M_g}^H(f)\mathbf{g}_{1,M_g}(f)e^{j2\pi fkT}df]$ and $\epsilon_{M_g}(k) \overset{\text{def}}{=} \text{Re}[\int \mathbf{w}_{M_g}^H(f)\boldsymbol{\epsilon}_{M_g}(f)e^{j2\pi fkT}df]$ is the

background noise (BN) component which is zero-mean Gaussian distributed with variance $\sigma^2_{\epsilon_{M_g}}$ whose expression is derived in Appendix C.

When the number of ISI and MUI terms at the output of the M-input WL MMSE receivers is large and when there are no dominant term in the ISI and MUI, an approximation of the central limit theorem (Lyapounov theorem [24, th. 27.3]) for independent non identically distributed r.v. can be applied and the SER is directly deduced from the SINR. For example, for BPSK symbols b_k and $b_{1,k}$, we get the approximation:

$$\mathrm{SER}_{M_g} \approx Q(\sqrt{\mathrm{SINR}_{M_g}}), \tag{45}$$

with $Q(x) \stackrel{\text{def}}{=} \int_x^{+\infty} \frac{1}{\sqrt{2\pi}} e^{-\frac{u^2}{2}} du$. This relation (45) confirms that the performance in term of output SINR and SER are equivalent.

When this number of ISI and MUI terms is weak and/or there is a dominant term in the ISI or MUI, the approximation is no longer valid, but an exact analytical expression of the SER can be derived. If $\mathcal{S}$ and $\mathcal{I}$ denote the sets of the ISI and MUI symbols, respectively, with respect to the symbol b_0, we now get by conditioning with respect to these BPSK symbols where $\mathcal{S} = \{-1,+1\}^{|\mathcal{S}|}$ and $\mathcal{I} = \{-1,+1\}^{|\mathcal{I}|}$:

$$\mathrm{SER}_{M_g} = \frac{1}{2^{|\mathcal{S}|}2^{|\mathcal{I}|}} \sum_{(..,b_{-1},b_{+1},..)\in\mathcal{S}} \sum_{(..,b_{1,-1},b_{1,0},b_{1,+1},..)\in\mathcal{I}} Q\left(\frac{u_{M_{g,0}} - (\sum_{k\neq 0} b_k u_{M_{g,k}} + \sum_k b_{1,k} u_{M_{1,g,k}})}{\sigma_{\epsilon_{M_g}}}\right). \tag{46}$$

B. Monte-Carlo experiments

When the conditions for which (45) can apply are not satisfied, we can resort to (46) for BPSK modulations. But this closed-form expression presents no engineering insights and shows that the SER and SINR are not directly related. To confirm that the results obtained in Sections V for output SINR are still vaild for output SER, we present in the following some Monte Carlo simulations.

B1) *One tap deterministic channels:* We consider the transmission of 1000 frames of 200 binary symbols ($b_k \in \{-1,+1\}$ and $b_{1,k} \in \{-1,+1\}$) and we assume, in this subsection, one tap deterministic channels which are constant over a frame and random from a frame to another. For each frame, we assume that $(\phi_{s,1}, \tau_1)$ are i.i.d. uniformly distributed on $[0, 2\pi] \times [0, 4T]$. Under these assumptions, Fig. 10 shows the variations of the SER given by the binary detector at the output of the different receivers for both R (BPSK) and QR ($\pi/2$-BPSK) signals, as a function of ϵ_s for $N = 1$, $\epsilon_1/\epsilon_s = 10$ dB and $\omega = 1$.

The results of Fig. 10 confirm, for both R and QR signals and from a SER perspective, the sub-optimality of the s and sc two-input receivers and the quasi-optimality of the s three-input receiver.

B2) *One tap Rayleigh channels:*

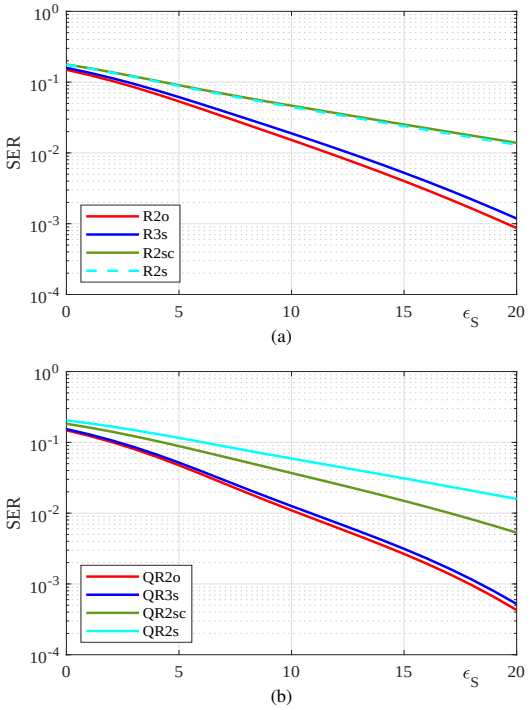

Fig. 10. SER as a function of ϵ_s ($N = 1$, $\epsilon_1/\epsilon_s = 10$ dB, $\omega = 1$, deterministic one tap channel, R (a) and $\pi/2$-ASK QR (b) signals

To complete the previous results and under the assumptions of Fig. 10, Fig. 11 shows the same variations as Fig. 10, but as a function of $\mathrm{E}(\epsilon_s)$ for Rayleigh fading channels for which $h(1)$ and $h_1(1)$ are zero-mean circular Gaussian independently distributed, such that $\mathrm{E}[\epsilon_1]/\mathrm{E}[\epsilon_s] = 10$ dB. The conclusions of Fig. 10 hold for Fig. 11.

VII. Conclusion

Additional insights, with respect to the companion paper [2], into WL MMSE receivers have been given in this paper, for both R and QR signals, omnipresent in numerous present and future applications, in the presence of data-like MUI and for propagation channels with or without delay spread. MSK and GMSK QR signals have been considered in this paper in addition to R and QR signals considered in [2]. Three WL MMSE receivers, corresponding to the optimal one (o), the one falsely assuming stationary MUI (s) and the one with a structure constraint (sc) mainly used in the literature, have been considered and analyzed in [2]. The (o) receiver requires the a priori knowledge of the MUI channels contrary to the (s) and (sc) receivers which only require the SOI channel, hence their practical interests. In the absence of MUI it has been shown in [2] that the (sc) WL MMSE receiver is sub-optimal with respect to the two other ones. In the presence of one MUI, channels with no delay spread and R signals, the (s) and (sc) WL MMSE receivers have been shown in [2] and this paper to be quasi-

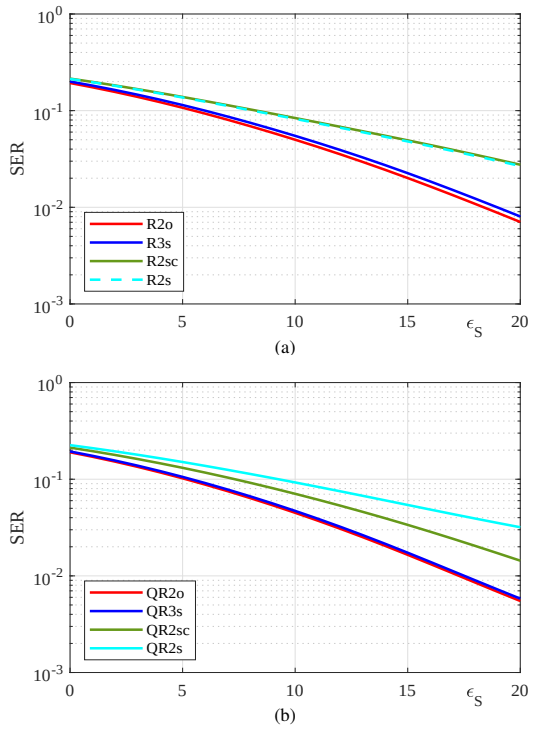

Fig. 11. SER as a function of $\mathrm{E}(\epsilon_s)$ ($N=1$, $\mathrm{E}(\epsilon_1)/\mathrm{E}(\epsilon_s)=10$ dB, $\omega=1$, Rayleigh fading one tap channel, R and $\pi/2$-ASK QR signals)

optimal for low values of the SRRC filter roll-off and sub-optimal with an increasing sub-optimality as the roll-off increases. In the same context, the (s) and (sc) WL MMSE receivers have been shown to be always sub-optimal for QR signals, whatever the constellation and the pulse shaping filter, showing the non equivalence of R and QR signals for WL MMSE receivers, due to different cyclostationarity properties of these signals. To improve the performance of the (s) WL MMSE receiver for both R and QR signals, a (s) three-input WL MMSE receiver has be proposed and analyzed, both analytically and by computer simulations, in this paper. This receiver exploits the cyclostationarity of the MUI and requires the knowledge of the SOI channel only. For both R and QR signals, the (s) three-input WL MMSE receiver has be shown to be quasi-optimal in most situations and to outperform both the (sc) and (s) two-input WL MMSE receivers. This interesting result open new perspectives for the implementation optimization of WL MMSE receivers in the presence of data-like MUI and, in particular, for the implementation of the (o) WL MMSE receivers from the only knowledge of the SOI channel.

APPENDIX

A. Proofs that the three-input optimal WL MMSE receiver reduces to two-input optimal WL MMSE receiver

Using the approach consisting to jointly estimate the SOI and MUI symbols $\mathbf{b}_n \overset{\text{def}}{=} [b_n, b_{1,n}, ..b_{P,n}]^T$, the filter $\mathbf{w}_3^*(-t)$ minimizing the MSE criterion corresponds to the first column of the $3N\times(P+1)$ matrix $\mathbf{W}_3^*(-t)$ filter whose output is $\mathbf{y}_3(t)=\mathbf{W}_3^H(-t)\otimes\mathbf{x}_3(t)$. This filter minimizes the joint MSE criterion: $\text{JMSE}=\mathrm{E}(\|\mathbf{b}_n-\mathbf{y}_3(nT)\|^2)$. Following the steps of the proof given in [23, Appendix A], where contrary to the two-input signal $\mathbf{x}_2(t)$, the CT background noise output $\mathbf{W}_3^*(-t)\otimes\boldsymbol{\epsilon}_3(t)$ is SO cyclostationary with cyclic frequencies $\alpha_i\in\{-\frac{1}{T},0,+\frac{1}{T}\}$, the JMSE criterion is given by:

$$\begin{aligned}\text{JMSE} &= \pi_b T\int_\Delta \mathrm{Tr}\big[\big(\mathbf{I}_{P+1}-\frac{1}{T}\sum_\ell \mathbf{W}_3^H(f-\frac{\ell}{T})\\ &\mathbf{G}_3(f-\frac{\ell}{T})\big)\big(\mathbf{I}_{P+1}-\frac{1}{T}\sum_\ell \mathbf{W}_3^H(f-\frac{\ell}{T})\mathbf{G}_3(f-\frac{\ell}{T})\big)^H\big]df\\ &+\int_\Delta \mathrm{Tr}\Big[\sum_{i=-1,0,+1}\sum_k \mathbf{w}_3^H(f-\frac{k}{T})\mathbf{R}_{\epsilon_3}^{\alpha_i}(f)\mathbf{w}_3(f-\frac{k+i}{T})\Big]df \quad (47)\end{aligned}$$

This JMSE is a quadratic functional of $\mathbf{W}_3(f-\frac{k}{T})$, $k\in\mathbb{Z}$. Following a standard method of the calculus of variations (see e.g., [25]), this JMSE (47) is minimized by the unique solution in $\mathbf{W}_3(f)$ of the following equation:

$$\begin{aligned}&\pi_b\mathbf{G}_3(f)\left[\mathbf{I}_{P+1}-\frac{1}{T}\sum_\ell \mathbf{G}_3^H(f-\frac{\ell}{T})\mathbf{W}_3(f-\frac{\ell}{T})\right]\\ &\quad=\sum_{i=-1,0,+1}\mathbf{R}_{\epsilon_3}^{\alpha_i}(f)\mathbf{W}_3(f-\alpha_i). \quad (48)\end{aligned}$$

Noting that $\sum_{i=-1,0,+1}\mathbf{R}_{\epsilon_3}^{\alpha_i}(f)\mathbf{W}_3(f-\alpha_i)=\mathbf{W}_3(f)+$ $+\begin{pmatrix}\mathbf{0}_{N,P+1}\\ \mathbf{W}_{3,3}(f+\frac{1}{T})\\ \mathbf{W}_{3,2}(f-\frac{1}{T})\end{pmatrix}$ with $\mathbf{W}_3(f)\overset{\text{def}}{=}\begin{pmatrix}\mathbf{W}_{3,1}(f)\\ \mathbf{W}_{3,2}(f)\\ \mathbf{W}_{3,3}(f)\end{pmatrix}$, it s straightforward to show that

$$\mathbf{W}_3(f)=\begin{bmatrix}\mathbf{G}_2(f)\mathbf{C}_{2_o}^d(f)\\ \mathbf{0}_{N,P+1}\end{bmatrix} \text{ is solution of (48).} \quad \blacksquare$$

B. Proofs of (33), (34)

To derive closed-form expressions of the SINR, it is easier to calculate the powers P_{SOI}, P_{ISI}, P_{MUI} and P_{BN} of the different terms of (44) than to use the global formula (26).

$$\text{SINR}_{3_s}=\frac{P_{\text{SOI}}}{P_{\text{ISI}}+P_{\text{MUI}}+P_{\text{BN}}}, \quad (49)$$

where the different powers are given by

$$P_{\rm SOI} = \pi_b \left[\int_\Delta \sum_k \mathbf{w}_{3_s}^H (f-\frac{k}{T}) \mathbf{g}_3 (f-\frac{k}{T}) df \right]^2 \quad (50)$$

$$\begin{aligned} P_{\rm ISI} &= \frac{\pi_b}{2T} \left(\int_\Delta |\sum_k \mathbf{w}_{3_s}^H (f-\frac{k}{T}) \mathbf{g}_3 (f-\frac{k}{T})|^2 df \right. \\ &+ \left. {\rm Re} \left[\int_\Delta (\sum_k \mathbf{w}_{3_s}^H (f-\frac{k}{T}) \mathbf{g}_3 (f-\frac{k}{T})) \right. \right. \\ &\left. \left. (\sum_\ell \mathbf{w}_{3_s}^H (-f-\frac{\ell}{T}) \mathbf{g}_3 (-f-\frac{\ell}{T})) df \right] \right) \\ &- \pi_b \left[\int_\Delta \sum_k \mathbf{w}_{3_s}^H (f-\frac{k}{T}) \mathbf{g}_3 (f-\frac{k}{T}) df \right]^2 \quad (51) \end{aligned}$$

$$\begin{aligned} P_{\rm MUI} &= \frac{\pi_b}{2T} \left(\int_\Delta |\sum_k \mathbf{w}_{3_s}^H (f-\frac{k}{T}) \mathbf{g}_{1,3} (f-\frac{k}{T})|^2 df \right. \\ &+ {\rm Re} \left[\int_\Delta (\sum_k \mathbf{w}_{3_s}^H (f-\frac{k}{T}) \mathbf{g}_{1,3} (f-\frac{k}{T})) \right. \\ &\left. \left. (\sum_\ell \mathbf{w}_{3_s}^H (-f-\frac{\ell}{T}) \mathbf{g}_{1,3} (-f-\frac{\ell}{T})) df \right] \right) \quad (52) \end{aligned}$$

$$\begin{aligned} P_{\rm BN} &= \frac{1}{2} \left(\sum_{\alpha \in A} \int \mathbf{w}_{3_s}^H (f+\frac{\alpha}{2}) \mathbf{R}_{\epsilon_3}^\alpha (f) \mathbf{w}_{3_s} (f-\frac{\alpha}{2}) \right. \\ &\left. + \sum_{\beta \in B} \int \mathbf{w}_{3_s}^H (f+\frac{\beta}{2}) \mathbf{C}_{\epsilon_3}^\beta (f) \mathbf{w}_{3_s}^* (-f+\frac{\beta}{2}) \right) \quad (53) \end{aligned}$$

where $A \stackrel{\rm def}{=} \{1/T, 0, +1/T\}$ and $B \stackrel{\rm def}{=} \{-1/T, 0\}$. Including the filter $\mathbf{w}_{3_s}(f)$ (16) in (50)-(53) allows us to derive after cumbersome algebraic manipulations:

$$P_{R,\rm SOI} = \frac{c^2}{\pi_b} \epsilon_s^2 \left(3 - \frac{|\alpha_{s,1}|^2 \epsilon_1}{1+\epsilon_1} - \frac{4|\alpha_{s,1}|^2 \epsilon_1 \cos^2 \phi_{s,1}}{1+2\epsilon_1} \right)^2 \quad (54)$$

$$P_{R,\rm ISI} = 0 \quad (55)$$

$$\begin{aligned} P_{R,\rm MUI} &= \frac{c^2}{\pi_b} |\alpha_{s,1}|^2 \epsilon_s \epsilon_1 \cos^2 \phi_{s,1} \left(\frac{4}{(1+2\epsilon_1)^2} \right. \\ &+ \left. \frac{1}{(1+\epsilon_1)^2} + \frac{4}{(1+\epsilon_1)(1+2\epsilon_1)} \right) \quad (56) \end{aligned}$$

$$\begin{aligned} P_{R,\rm BN} &= \frac{c^2}{\pi_b} \frac{\epsilon_s}{2} \left(9 + |\alpha_{s,1}|^2 \epsilon_1 \left(\frac{\epsilon_1}{(1+\epsilon_1)^2} \right. \right. \\ &- \left. \left. \frac{6}{1+\epsilon_1} - \frac{8(2\epsilon_1^2+6\epsilon_1+3)}{(1+2\epsilon_1)^2)(1+\epsilon_1)} \cos^2 \phi_{s,1} \right) \right) \quad (57) \end{aligned}$$

with

$$c \stackrel{\rm def}{=} \pi_b \left(1 + \epsilon_s \left(3 - \frac{|\alpha_{s,1}|^2 \epsilon_1}{1+\epsilon_1} - \frac{4|\alpha_{s,1}|^2 \epsilon_1 \cos^2 \phi_{s,1}}{1+2\epsilon_1} \right) \right)^{-1} \quad (58)$$

for R signals and

$$\begin{aligned} P_{QR,\rm SOI} &= \pi_b \left(1 - \frac{1}{2\pi_b} (c_1 + c_2) \right)^2 \\ &= \frac{\epsilon^2}{4\pi_b} \left[c_1 \left(3 - \frac{|\alpha_{s,1}|^2 \epsilon_1}{1+\epsilon_1} - \frac{4|\alpha_{s,1}|^2 \epsilon_1 \cos^2 \zeta_{s,1}}{1+2\epsilon_1} \right) \right. \\ &+ \left. c_2 \left(3 - \frac{|\alpha_{s,1}|^2 \epsilon_1}{1+\epsilon_1} - \frac{4|\alpha_{s,1}|^2 \epsilon_1 \cos^2 \psi_{s,1}}{1+2\epsilon_1} \right) \right]^2 \quad (59) \end{aligned}$$

$$\begin{aligned} P_{QR,\rm ISI} &= \frac{\epsilon^2}{2\pi_b} \left[c_1 \left(3 - \frac{|\alpha_{s,1}|^2 \epsilon_1}{1+\epsilon_1} - \frac{4|\alpha_{s,1}|^2 \epsilon_1 \cos^2 \zeta_{s,1}}{1+2\epsilon_1} \right) \right. \\ &- \left. c_2 \left(3 - \frac{|\alpha_{s,1}|^2 \epsilon_1}{1+\epsilon_1} - \frac{4|\alpha_{s,1}|^2 \epsilon_1 \cos^2 \psi_{s,1}}{1+2\epsilon_1} \right) \right]^2 \quad (60) \end{aligned}$$

$$\begin{aligned} P_{QR,\rm MUI} &= \frac{c_1^2}{2\pi_b} |\alpha_{s,1}|^2 \epsilon_s \epsilon_1 \cos^2 \zeta_{s,1} \left(\frac{4}{(1+2\epsilon_1)^2} \right. \quad (61) \\ &+ \left. \frac{1}{(1+\epsilon_1)^2} + \frac{4}{(1+\epsilon_1)(1+2\epsilon_1)} \right) \\ &+ \frac{c_2^2}{2\pi_b} |\alpha_{s,1}|^2 \epsilon_s \epsilon_1 \cos^2 \psi_{s,1} \left(\frac{4}{(1+2\epsilon_1)^2} \right. \quad (62) \\ &+ \left. \frac{1}{(1+\epsilon_1)^2} + \frac{4}{(1+\epsilon_1)(1+2\epsilon_1)} \right) \quad (63) \end{aligned}$$

$$\begin{aligned} P_{QR,\rm BN} &= \frac{c_1^2}{\pi_b} \frac{\epsilon_s}{4} \left(9 + |\alpha_{s,1}|^2 \epsilon_1 \left(\frac{\epsilon_1}{(1+\epsilon_1)^2} \right. \right. \\ &- \left. \left. \frac{6}{1+\epsilon_1} - \frac{8(2\epsilon_1^2+6\epsilon_1+3)}{(1+2\epsilon_1)^2)(1+\epsilon_1)} \cos^2 \zeta_{s,1} \right) \right) \\ &+ \frac{c_2^2}{\pi_b} \frac{\epsilon_s}{4} \left(9 + |\alpha_{s,1}|^2 \epsilon_1 \left(\frac{\epsilon_1}{(1+\epsilon_1)^2} \right. \right. \\ &- \left. \left. \frac{6}{1+\epsilon_1} - \frac{8(2\epsilon_1^2+6\epsilon_1+3)}{(1+2\epsilon_1)^2)(1+\epsilon_1)} \cos^2 \psi_{s,1} \right) \right) \quad (64) \end{aligned}$$

with

$$c_1 \stackrel{\rm def}{=} \pi_b \left(1 + \epsilon_s \left(3 - \frac{|\alpha_{s,1}|^2 \epsilon_1}{1+\epsilon_1} - \frac{4|\alpha_{s,1}|^2 \epsilon_1 \cos^2 \zeta_{s,1}}{1+2\epsilon_1} \right) \right)^{-1} \quad (65)$$

$$c_2 \stackrel{\rm def}{=} \pi_b \left(1 + \epsilon_s \left(3 - \frac{|\alpha_{s,1}|^2 \epsilon_1}{1+\epsilon_1} - \frac{4|\alpha_{s,1}|^2 \epsilon_1 \cos^2 \psi_{s,1}}{1+2\epsilon_1} \right) \right)^{-1} \quad (66)$$

for QR signals. From the expressions (54)-(66), we see that for $\tau_1 = 0$, $\cos^2 \psi_{s,1} = \cos^2 \zeta_{s,1}$, which implies $c_1 = c_2 = c$ and thus the powers of the different components of $z_{3_s}(k)$ for R and QR signals are equal and the associated SINR are equal. ■

C. Proofs of expressions of $\sigma^2_{\epsilon_{M_g}}$

For the (o) and (s) receivers with $M = 1, 2$ inputs, $\sigma^2_{\epsilon_{M_g}} = \frac{MN_0}{2} \int \|\mathbf{w}_{M_g}(f)\|^2 df$ and for the (sc) receiver $\sigma^2_{\epsilon_{M_{sc}}} = \frac{MN_0}{2} \int |v(f)|^2 \|\mathbf{w}_{M_{sc}}(f)\|^2 df$ for R signals and $\sigma^2_{\epsilon_{M_{sc}}} = \frac{MN_0}{2} \int |v(f+4/T)|^2 \|\mathbf{w}_{M_{sc}}(f)\|^2 df$ for QR signals. For the three-input receiver $\sigma^2_{\epsilon_{3_s}}$ is given by (53) where $\mathbf{R}_{\epsilon_3}^\alpha(f)$ and $\mathbf{C}_{\epsilon_3}^\beta(f)$ come from (27) and (28), respectively. ■

REFERENCES

[1] B. Picinbono and P. Chevalier, "Widely linear estimation with complex data," *IEEE Trans. Signal Process.*, vol. 43, no. 8, pp. 2030-2033, Aug. 1995.

[2] P. Chevalier, J.-P. Delmas, and R. Lamberti, "New insights into widely linear MMSE receivers for communication networks using data-like rectilinear or quasi-rectilinear signals - Part I: One and two-input receivers", *IEEE Trans. Vehicular Technology* submitted, Nov. 2023.

[3] W. Deng, Z. Li, Y. Xia, K. Wang, and W. Pei, "A Widely linear MMSE Anti-Collision method for multi-antenna RFID readers," *IEEE Commun. Letters*, vol 23, no. 4, pp. 664-647, Aug. 2019.

[4] R. Gui, N.M. Balasubramanya, and L. Lampe, "Connectivity performance evaluation for grant-free narrowband IoT with widely linear receivers," *IEEE Internet of Things Journal*, vol 7, no. 10, pp. 10562-10572, Oct. 2020.

[5] D.J. Nelson and J.R. Hopkins, "Coherent demodulation of AIS-GMSK signals in co-channel interference," *IEEE Asilomar Conf. on Circuits, Systems and Computers*, Nov. 2011.

[6] G.M. Swetha, K. Hemavathy, S. Natarajan, and V. Sambasiva, "Overcome message collisions in satellite automatic ID systems, *Microwave and RF, Systems*, May. 2018.

[7] O. Cherrak, H. Ghennioui, N. Thirion-Moreau, and E.H. Abarkan, "Blind separation of complex-valued satellite-AIS data for maritime surveillance : a spatial quadratic time-frequency domain approach," *International Journal of Electrical and Computer Engineering (IJECE)*, pp. 1732-1741, June. 2019.

[8] M. Bavand and S.D. Blostein, "User selection and multiuser widely linear precoding for one-dimensional signalling," *IEEE Trans. Vehicular Technology*, vol. 67, no. 12, pp. 11642-11653, Dec. 2018.

[9] S. Javed, O. Amin, B. Shihada, and M.S. Alouini, "A journey from improper Gaussian signaling to asymetric signaling," *IEEE Commun. Surveys and Tutorials*, vol. 22, no. 3, pp. 1539-1591, Third Quarter 2020.

[10] D. Tong, Y. Ding, Y. Liu, and Y. Wang, "A MIMO-NOMA framework with complex-valued power coefficients," *IEEE Trans. Vehicular Technology*, vol. 68, no. 3, pp. 2244?-259, March 2019.

[11] J.C. De Luna Ducoing, N. Yi, Y. Ma, and R. Tafazolli, "Using real constellations in fully-and over loaded large MU-MIMO systems with simple detection", *IEEE Wireless Commun. Letters*, vol. 5, no. 1, pp. 92-95, Feb. 2016.

[12] D. Darsena, G. Gelli, I. Iudice, and F. Verde, "Equalization techniques of control and non-payload communication links for unmanned aerial vehicles," *IEEE Access*, vol. 6, pp. 4485-4496, 2018.

[13] B. Farhang-Boroujeny and R. Kempter, "Multicarrier communication techniques for spectrum sensing and communication in cognitive radios," *IEEE Commun. Mag.*, vol. 46, no. 4, pp. 80-85, Apr. 2008.

[14] D. Chen, Y. Tian, D. Qu, and T. Jiang, "OQAM-OFDM for wireless communications in future internet of things: a survey on key technologies and challenges," *IEEE Internet of Things Journal*, vol. 5, no. 5, pp. 3788-3809, Oct. 2018.

[15] P. Chevalier, R. Chauvat, and J.-P. Delmas, "Enhanced widely linear filtering to make quasi-rectilinear signals almost equivalent to rectilinear ones for SAIC/MAIC," *IEEE Trans. Signal Proces.*, vol. 66, no. 6, pp. 1438-1453, March 2018.

[16] P. Chevalier, R. Chauvat, and J.-P. Delmas, "Widely linear FRESH receivers for cancellation of data-like rectilinear and quasi-rectilinear Interference with frequency-offsets", *Signal Processing*, vol 188, pp. 1-13, 108171, Nov., 2021.

[17] P.A. Laurent, "Exact and approximate construction of digital phase modulations by superposition of amplitude modulated pulses (AMP)", *IEEE Trans. Commun.*, vol. 34, no. 2, pp. 150-160, Feb. 1986.

[18] H. Trigui and D.T.M. Slock, "Performance bounds for cochannel interference cancellation within the current GSM standard," *Signal Proccess., Elsevier*, vol. 80, pp. 1335-1346, 2000.

[19] W.A. Gardner, W.A. Brown, and C-K. Chen, "Spectral correlation of modulated signals: Part II - Digital modulation", *IEEE Trans. commun.*, vol. 35, no. 6, pp. 595-601, June 1987.

[20] P. Gournay and P. Viravau, "Corrélation spectrale théorique des modulations CPM, Partie I: Résultat analytique pour les modulations CPFSK à 2 états (1-Rec)", *Annals of Telecom.*, vol 53, no. 7-8, pp. 267-278, 1998.

[21] D. Vucic and M. Obradovic, "Spectral correlation evaluation of MSK and offset QPSK modulation", *Signal Processing*, vol 78, pp. 363-367, 1999.

[22] W. Gardner, "Cyclic Wiener filtering: theory and method," *IEEE Trans. commun.*, vol. 41, no. 1, pp. 151-163, Jan. 1993.

[23] P. Chevalier, J.-P. Delmas, and R. Lamberti, "New insights into widely linear MMSE receivers for communication networks using data-like rectilinear or quasi-rectilinear signals - Part I: one and two-inputs receivers", complete paper, available at https://hal.science/hal-04268020.

[24] P. Billingsley, *Probability and measure*, second edition, John Wiley and Sons, New-York, 1986.

[25] P. Balaban and J. Saltz, "Optimum diversity combining and equalization in digital transmission with applications to cellular mobile radio - Part I: theoretical considerations", *IEEE Trans. commun.*, vol. 40, no. 5, pp. 885-894, May 1992.